Hemispheric Asymmetries in Perceptual-Motor Processing and the Space-Ship Plot:

Simple Reaction Time to Lateralised Sinusoidal Gratings

Nicholas P Holmes[1]

BSc (Hons.), Psychology and Neuroscience

Supervisors: Dr Ian J Murray[2] and Dr Nuala Brady[1]

Submitted 12th May, 2000

[1] Department of Psychology, The University of Manchester
[2] Department of Optometry and Neuroscience, The University of Manchester Institute of Science and Technology

Contents

1. Abstract

Simple reaction time (RT) to sinusoidal gratings varying in contrast, spatial frequency and luminance was measured for brief stimuli presented at different eccentricities in both visual fields of two young subjects. Over a range of contrasts, RT increased in proportion to the reciprocal of contrast. With increasing eccentricity and spatial frequency, the slope and constant of the hyperbolic RT-contrast curve increased. With decreases in luminance, the constant but not the slope increased. The linear relationship between RT and the reciprocal of contrast held for all spatial and luminance stimulus-characteristics. One subject showed no consistent trend towards lateralisation of processing as a function of stimulus characteristics. The other subject showed a consistent and highly significant left visual field / right hemisphere advantage (13 to 19 ms) over all stimulus conditions. Control experiments for one subject indicated a highly significant left versus right foot advantage, and an 80 ms advantage for hand over foot responses.

A linear coefficient relating the RT to the reciprocal of contrast was calculated for all stimulus conditions, and plot on a single graph for each subject. The slope coefficient varied monotonically as a function of eccentricity for high luminance stimuli at all spatial frequencies. The slope coefficient was constant for scotopic luminance conditions. Aspects of this 'Space-Ship' plot were related to electrophysiological and neuroanatomical characteristics of the visual input pathways. The RT-1/contrast slope coefficient predicts contrast gain and contrast sensitivity in single unit primate studies. For this reason, the slope coefficient is suggested as a superior alternative to absolute RT data, in assessing the hemispheric-asymmetrical processing of sinusoidal gratings in the simple reaction time paradigm.

2. Introduction

The paradigmatic approach to studying visual hemispheric asymmetries involves the presentation of stimuli tachistoscopically to left and right visual hemifields (and therefore selectively to the right and left hemisphere respectively; though see Ivry and Robertson, 1998), while requiring the subject to perform a task contingent on the stimulus. Task performance speed or accuracy is taken as a behavioural measure of visual perceptual processing. This behavioural measure is compared for stimuli presented to the left and right hemispheres, and any differences are taken as evidence of hemispheric processing asymmetries. In some early studies, researchers presented stimuli consisting of information at two spatial scales in normal subjects' visual fields (see Figure 1, below). These experiments tended to show that stimuli presented in the left visual field (LVF) were processed more efficiently if the required (target) information was contained at the relatively larger ('global') spatial scale. Conversely, processing of stimuli in the right visual field (RVF), was relatively more efficient for information at the smaller ('local') spatial scale.

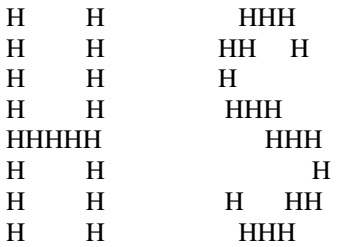

Figure 1. Example of Navon's (1977) hierarchical stimuli*. Both figures show two spatial scales of information. The figure on the left contains the target 'H' at both local (detail) and global (overall) levels. The figure on the right contains the target 'H' at the local level, and the distractor 'S' at the global level. Navon showed that letters at the global scale were detected more quickly than letters at the local scale. Later studies using similar stimuli (e.g. Martin, 1979) found that for stimuli presented in the LVF, the global scale information was detected relatively more quickly than the local information. For RVF stimuli, the opposite was true.*

The findings from experiments with normal subjects converged with data from brain-damaged patients. In patients with left hemisphere (LH) damage, local-level processing was relatively more impaired than global-level processing, and in patients with right hemisphere (RH) damage, global processing was relatively more impaired (although see Marshall and Halligan, 1995; Fendrich and Gazzaniga, 1990; and Polster and Rapcsak, 1994 for qualifications). Sergeant (1983) reviewed studies of hemispheric processing asymmetries and formulated the spatial frequency hypothesis. She claimed that the

hemispheres are specialised for processing visual information at different spatial scales. The LH is specialised for (local-level) high spatial frequency (SF) information, while the RH processes (global-level) low spatial frequencies more efficiently[3]. Stimulus manipulations that tend to decrease the *availability* of high frequency information, such as blurring, increasing stimulus eccentricity, or decreasing stimulus duration, will tend to bias processing towards a RH advantage in a task-dependent manner (but see Hellige, 1986; Christman, 1990; Peterzell, 1991 for the Information-Energy Hypothesis). Conversely, processing is biased towards the LH by removing low spatial frequencies (Ivry and Robertson, 1998).

Visual laterality research since these early studies and the formulation of the spatial frequency hypothesis has tended to support the LH-local and RH-global processing dichotomy (van Kleek, 1989), but with some qualifications. Firstly, global and local levels can not be defined in absolute terms such as stimulus size or angle of arc, rather the asymmetries arise between global and local scales *relative to the stimuli* and the nature of the task (Polich, 1978; Kinchla and Woolfe, 1979; Christman *et al*., 1991). Secondly, and importantly for the present study, processing asymmetries are consistently found for tasks requiring the *identification* of or *discrimination* between different stimuli (e.g. Kitterle *et al*., 1990; Kitterle and Selig, 1991; Kitterle *et al*., 1992; Proverbio *et al*., 1997; Niebauer and Christman, 1999), while stimulus *detection* tasks (simple reaction time or two-interval forced-choice detection) do not yield processing asymmetries (Rose, 1983; Fiorentini and Berardi, 1984; Kitterle and Kaye, 1985; Peterzell *et al*., 1989).

This has led researchers to question the basis of hemispheric processing asymmetries. The necessary computations required for simple reaction time (SRT) and detection tasks are assumed to occur and be completed 'early' in visual processing; to require only pre-attentive processing that is dependent primarily on the neurophysiology of retino-geniculo-striate projections (McKeever and Hoff, 1979). On the other hand, tasks requiring identification, discrimination, or comparison of stimuli require attentive processing, and are mediated by extra-striate and parieto-temporal cortex, as supported by lesion studies (Fink *et al*., 1996; Ivry and Robertson, 1998). It is assumed that attention

[3] The spatial frequency of a stimulus is defined as the reciprocal of the angular subtense at the eye of one complete period of luminance modulation (cycles per degree; cpd), measured perpendicularly to an iso-luminance contour for simple gratings.

mediates processing at 'higher,' 'cognitive' levels, while pre-attentive processing is constrained by neuroanatomy, is serial, and domain-specific (in accord with the modularity thesis; Fodor, 1983).

It follows that, since there are no anatomical hemispheric asymmetries in the retino-striate projections (Braun *et al*, 1996; but see Rao *et al*., 1981), there consequently should be no functional asymmetries for SRT tasks. Research on functional asymmetries for SRT tasks has not entirely supported this conclusion, however.

One problem in interpreting SRT studies is that any asymmetries in reaction time are likely to be very small. It is therefore hard to find statistically significant results given the intra- and inter-subject variation in reaction times (e.g. Greenlee and Breitmeyer, 1989). Secondly, the transfer of information from the hemisphere receiving the stimulus, to the hemisphere responsible for the initiation of the motor response takes time. It is assumed that if the LH both receives the stimulus and initiates the response (i.e. a RVF stimulus and right hand response, or LVF and left hand), the *intra*-hemispheric visuo-motor conduction time is shorter than that for a response with the hand ipsilateral to the receiving hemisphere (requiring *inter*-hemispheric visuo-motor conduction). By subtracting the shorter, uncrossed RT from the longer, crossed RT, an estimate of the inter-hemispheric transmission time (IHTT) is obtained. The value of IHTTs consistently are between 1 and 3 ms (Clarke and Zaidel, 1989; Braun and Daigneault, 1994).

Estimates of the IHTT are usually obtained with small, aperiodic, flashed stimuli of a fixed luminance presented at one eccentricity in both visual fields, and requiring a SRT response. Such studies have found fairly consistent RH advantages between 1.3 and 10 ms, after the extra IHTT time is taken into account, and despite right-handed subjects responding with their left hand on half of the trials (e.g. Anzola *et al*., 1977; Berlucchi *et al*., 1977; Davidoff, 1977; McKeever and Hoff, 1979; Brown *et al*., 1984). These RH advantages have been interpreted in terms of the LH-verbal, RH-perceptual/spatial dichotomy (see Ivry and Robertson, 1998). Left hemisphere SRT advantages have also been reported (e.g. DiStefano *et al*., 1980; Lines and Milner, 1983; Lines *et al*., 1984), but of the published studies these are in the minority.

The results from studies using lateralised flash stimuli should be borne in mind when

interpreting SRT data for more complex stimuli. Sinusoidal grating stimuli, where the luminance of the stimuli varies according to a sinusoidal function, are the paradigmatic stimuli for studying early processing. Early visual perception can be characterised as achieving an analysis of the visual scene into spatial spectral components (according to the Fourier analogy; Campbell and Robson, 1968), this analysis proceeding via separate 'channels,' each sensitive to a narrow (about 1 – 1.4 octaves; DeValois *et al*., 1982) range of spatial frequencies. Stimuli varying periodically (typically in the horizontal direction) will selectively be processed by channels according to their spatial frequency. The optimal stimulus for these channels is considered to be sinusoidal or square-wave gratings, and simple detection paradigms take either reaction time or detection threshold as a behavioural measure of the channel's output.

Yund and colleagues (1990) demonstrated a significant RVF-LH advantage for the detection of simple square-wave gratings when presented among distractors. Rao and colleagues (1981) suggested that the RH was more sensitive to static or slowly moving gratings, while the LH favoured moving and flickering gratings. These results were interpreted in terms of a possible asymmetry of retino-geniculate sustained (RH) and transient (LH) channel projections. Their preliminary report was not followed up, however, and Braun and colleagues (1996) question the basis of a neuroanatomical projection asymmetry.

Interpretation of grating detection measures requires that several stimulus parameters are taken into account. The threshold for grating detection, defined as the minimum luminance modulation (i.e. grating contrast, see below) required to detect 50% of stimulus presentations (or 75% in a two-alternative, forced-choice paradigm), varies non-monotonically as a function of the spatial frequency of the grating. Grating contrast is calculated according to Michelson (1927), as the difference between the maximum and minimum grating luminance, divided by twice the mean luminance, as in Equation 1 and Figure 2A, below.

$$\text{Michelson contrast, } C = (L_{max} - L_{min})/ (2L_{mean}) \qquad \text{(Equation 1)}$$

The contrast sensitivity function (CSF) plots contrast sensitivity (1/contrast threshold) against spatial frequency, and typically shows peak sensitivity at 2 to 5 cpd, with

sensitivity falling off either side of this range (see Figure 2B, below; Campbell and Robson, 1968).

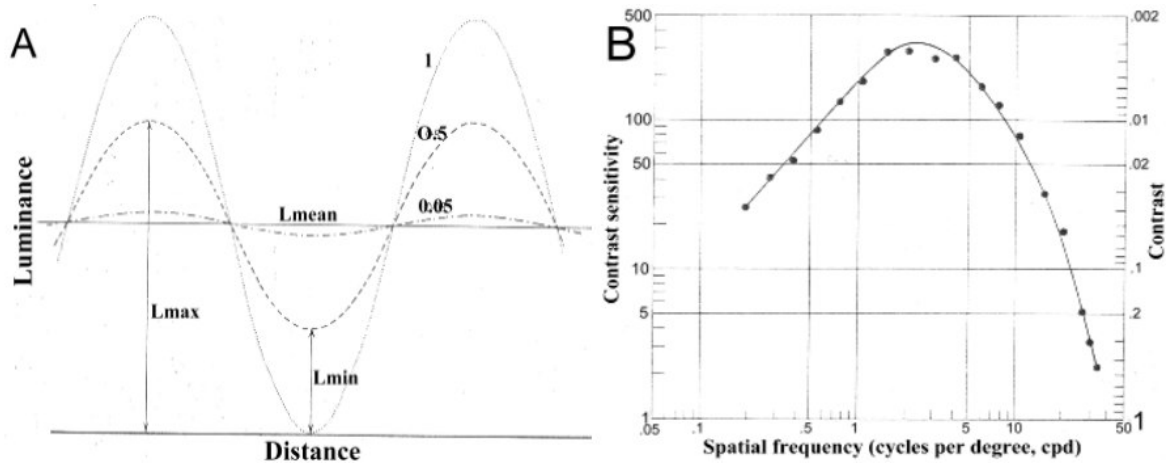

Figure 2. Contrast and the contrast sensitivity function (CSF). A*. Michelson contrast is defined as the difference between the maximum and minimum luminance ($L_{max} - L_{min}$), divided by twice the mean luminance ($2L_{mean}$) for gratings with luminance varying periodically over distance. Three example sinusoidal luminance profiles are given (with contrast = 1, 0.5, and 0.05).* ***B****. The CSF for high luminance, foveal sinusoidal gratings. The reciprocal of the contrast at which only 50% of stimuli are detected is plot against the spatial frequency of the grating. Optimal contrast sensitivity (1/threshold) is found for gratings of 2 – 5 cpd, while sensitivity drops off rapidly either side of this value. The overall CSF function reflects not the individual sensitivity of cells tuned to spatial frequencies, but rather the overall frequency distribution of tuned cells (*Campbell and Robson, 1968; DeValois et al., 1982*). Figures are adapted from* Campbell and Green, 1965 *(A), and* Campbell and Maffei, 1975 *(B).*

Due to optical imperfections of the eye apparent, subjective contrast is lower than the physical contrast of the stimulus (Campbell and Robson, 1968). Furthermore, apparent contrast is greater for high than low spatial frequencies (Franzén, 1975), and increases with eccentricity (Bryngdahl, 1966). For gratings sufficiently high in contrast, however, contrast constancy operates over a wide range of spatial frequencies (Georgeson and Sullivan, 1975; Kulikowski, 1976; Brady and Field, 1995).

The CSF is also affected by grating luminance and eccentricity. With decreasing luminance and increasing eccentricity, the peak sensitivity of the CSF shifts both to lower spatial frequencies, and to an *absolutely* lower sensitivity (a diagonal shift downwards and to the left in Figure 2B). Both of these effects decrease the overall bandwidth of the CSF (Rijsdijk *et al*., 1980; Kroon *et al*., 1980). The effects of eccentricity and luminance reflect the progressive loss of the output of individual channels; the loss of high spatial frequency channels occurring before low spatial frequency channels.

Contrast, spatial frequency, eccentricity and luminance have differential and interacting effects on SRT. Different gratings are not, therefore, directly comparable to each other without regard to all these factors. Hemispheric asymmetries in SRT can not reliably be compared as a function of spatial frequency, say, since gratings of different spatial frequency are not equivalent in stimulus energy,[4] at least for low contrast stimuli (Plainis, 2000, personal communication). One way of characterising a stimulus in order to achieve comparisons between gratings is in terms of its distance from contrast threshold. In a detection paradigm, stimuli of different spatial frequency could be presented at a fixed contrast, say 1 log unit, above threshold. Another method of equating stimuli with different spatial or luminance characteristics, is to use detection reaction times. Two stimuli are said to be equivalent, then, if they have equal SRTs. A stimulus of 2 cpd and 0.05 contrast, for example, might be equivalent to one of 5 cpd and 0.1 contrast. Evoked potential data could also be used in this respect (see Campbell and Maffei, 1975).

The distance-from-threshold, and iso-RT considerations take only the x- and y-axes on the plot of RT against contrast into consideration respectively. It is not the case, however, that a given modulation of contrast results in the same modulation of reaction time for all conditions, however (see Harwerth and Levi, 1978). Rather, the increase in RT contingent on decreases in stimulus contrast is greater for high than low spatial frequencies, for more eccentric stimuli, for less luminant stimuli, and for shorter stimulus presentations. It may therefore be preferable to derive a measure that is sensitive both to contrast and reaction time, in order to assess the equivalence of suprathreshold and near-threshold stimuli with different spatial or luminance characteristics.

The present study has three primary aims. 1. To evaluate the effect on SRT of a wide range of stimulus contrasts (C = 0.5 to 0.006), eccentricities (0º, 5º, 10º, 15º), spatial frequencies (0.5, 1.73, 5.61 cpd), and luminances (0.02, 0.2, 20 $cd.m^{-2}$). 2. To determine if there are systematic hemispheric asymmetries for SRT as a function of the manipulated stimulus parameters. 3. To derive a RT-contrast coefficient in order that supra- and near-threshold stimuli with different spatial or luminance characteristics can more reliably be compared in SRT measures of hemispheric processing asymmetries, particularly with respect to the differential hemispheric processing of spatial frequencies.

[4] That is, stimulus energy with respect to perceptual processing speed or efficiency.

3. Methods

3.1 Subjects

Two right-handed male subjects aged 23 (NH) and 29 (SP), with corrected-to-normal vision participated in the experiment. Subject NH was the author; subject SP was highly experienced with visual RT studies. Both subjects were aware of the purpose and background of the study.

3.2 Stimuli

Vertical gratings with a sinusoidally-varying luminance profile were generated on a high resolution Red-Green graphics display monitor (Barco, CCID 7651). The gratings were composed of separate red and green components, combined in phase and in equal proportion (equal luminance) to produce achromatic ('yellow,' 585 nm) sinusoidal gratings. Screen hue and mean luminance (20, 0.2, or 0.02 $cd.m^{-2}$) remained constant throughout stimulus presentations. The monitor screen was occluded by opaque black card except for a central circular aperture of diameter 14 cm, equating to 7º of visual angle at the viewing distance of 114 cm. Stimuli were viewed binocularly. A small (4 mm) black cross was provided at the centre of the screen as a fixation point (foveal conditions). For eccentric conditions a dim red LED (5 mm diameter) was positioned along the horizontal meridian at 5º, 10º, or 15º from the centre of the screen in either visual field (see Figure 3, below).

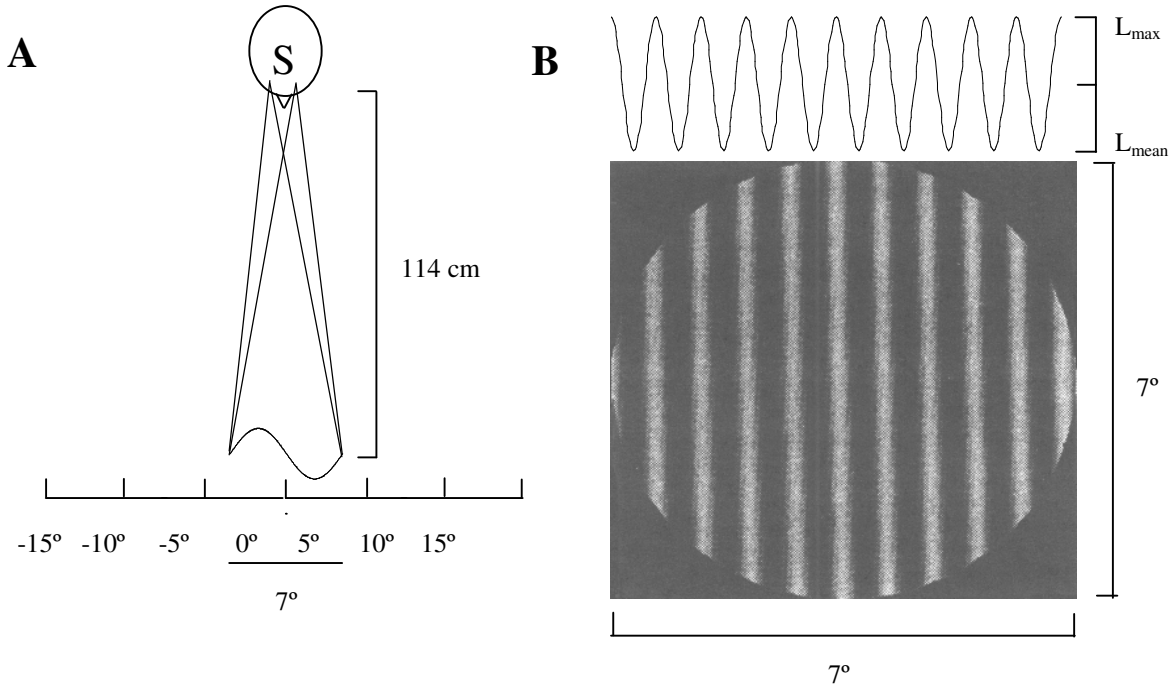

Figure 3. The experimental set-up and example stimulus. ***A***. *The subject, S, sat 114 cm from the centre of the stimulus field, denoted by the sine-wave subtending 7º of arc. A small fixation cross was provided at the centre of the screen (0º). Red LEDs were positioned at 5º, 10º, and 15º in both visual fields, and served as fixation points for eccentric conditions. Stimuli were viewed binocularly.* ***B***. *An example (from* Plainis, 1999*, using the same apparatus) sinusoidal grating, of 10/7 cpd (at 114 cm) and high contrast. The sinusoidal function at the top of the figure illustrates the stimulus luminance profile, and is in-phase with the example grating. Mean luminance and Michelson contrast (modulation depth, or amplitude) were calculated from* L_{max} *and* L_{min} *values.* L_{mean} *remained constant.*

Stimuli of 340 ms duration varied in mean luminance (20, 0.2 and 0.02 cd.m^{-2}), spatial frequency (0.5, 1.73, and 5.61 cpd), and contrast (10 levels between 0.5 and 0.006), and were presented foveally, or peripherally at varying eccentricity (with the centre of the stimulus at 5º, 10º, or 15º) in both right and left hemifields. Stimulus onset and offset followed a square-wave step function and was complete within the monitor frame refresh time (approximately 10 ms).

Monitor luminance was calibrated at the outset, and tested with a 1º spot photometer (Photo Research 1500; Micron, London) prior to each experimental session. Screen luminance in photopic conditions was 20 ± 1 cd.m^{-2} (mean ± SEM across experimental sessions). Stimulus luminances of 0.2 ± 0.02 cd.m^{-2} and 0.02 ± 0.002 cd.m^{-2} were achieved by placing neutral density filters over the screen, and adjusting the nominal screen luminance through the PC software interface. Screen luminance was maintained within the linear portion of the monitor calibration curve (curve not shown).

Nominal (software value) versus measured (using spot-photometer) Michelson contrast was determined for nominal contrast values of 1 to 0.02 (contrasts below 0.02 were immeasurable with the spot photometer) for square-wave gratings of 0.2 and 2 cpd. The resulting contrast calibration curves are given in Figure 4 below.

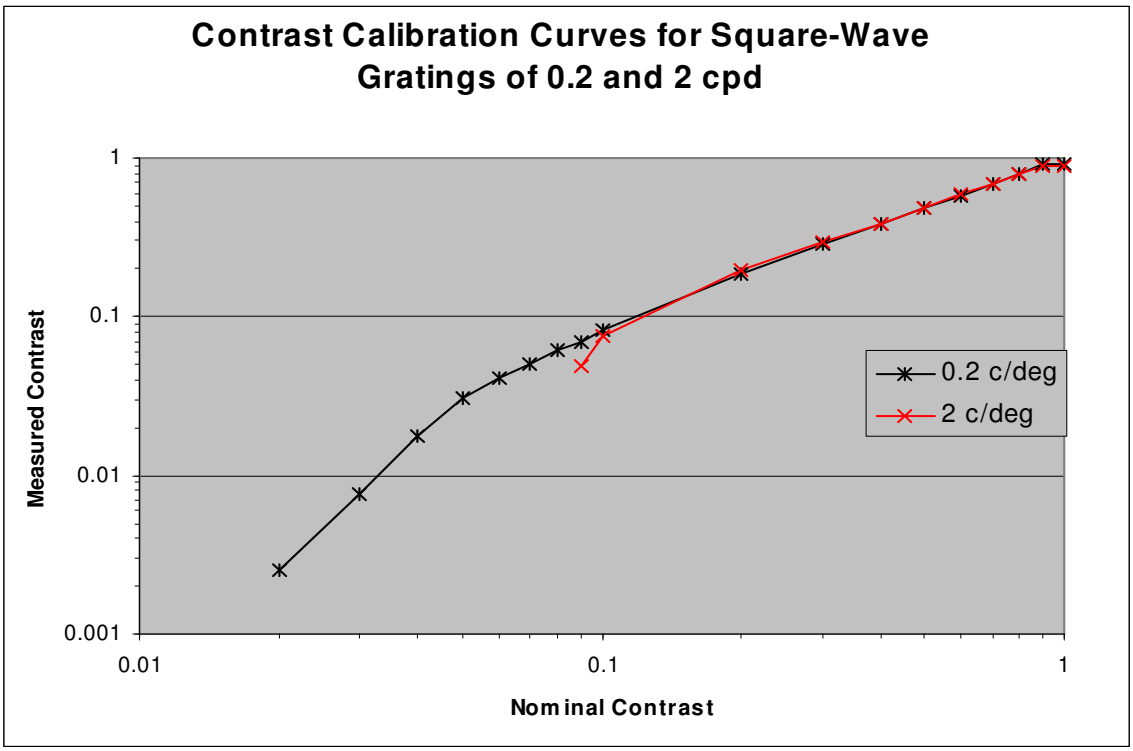

Figure 4. Contrast calibration curves*. Michelson contrast was calculated for square-wave gratings of 0.2 (black) and 2 (red) cpd, over a range of nominal contrasts (C = 1 to 0.02). The calibration curves are highly linear over the range C = 0.9 to 0.05 (r^2 = 0.9998; y = 1.025x - 2.15). Departure from linearity below C = 0.1 (2 cpd) and 0.05 (0.2 cpd) reflects the limited sensitivity of the spot-photometer.*

Michelson contrast levels below C = 0.05 were not reliably measurable with the spot-photometer. However, grating-detection RTs continued to be contrast-modulated at contrasts as low as C = 0.006 with optimal (low spatial frequency, high luminance) stimulus conditions. It can be assumed that nominal contrast varied proportionally with stimulus contrast at all contrast levels. The nature of this relationship below C = 0.05, however, was not determinable.

3.3 Apparatus

Stimuli were generated and controlled by a Millipede Prisma VR1000, 12-bit generator card in a 386 SX IBM-compatible personal computer. This enabled the luminance of 900 vertical raster lines to be set independently between 0 and 80 cd.m^{-2} in 0.1 cd.m^{-2} steps.

The red, green, and synchronisation inputs to the monitor were controlled by the generator card through a Prisma software interface. At stimulus onset, a CED 1401 controller card in the PC sent a trigger signal to a CED 1401 smart interface (Cambridge Electronic design, Ltd.) which started a millisecond-resolution timer. Response buttons were connected to a second input to the 1401 interface. Subject's responses stopped the timer; the reaction time was recorded to the nearest millisecond, and the result was output to a text file stored on the PC hard drive.

Response buttons were attached to the end of the right arm of the subject's chair, positioned to allow the subject's hand and forearm to rest comfortably, with the forefinger on the button. For foot RT control experiments (see below), a Treadlite foot pedal (Linemaster, Woodstock), was positioned on the floor 50 cm infront of the chair.

3.4 Procedure

Subjects sat with their head positioned 114cm from the screen, with the centre of the stimulus field at eye level. Lights were turned off, and a heavy curtain was drawn around the subject and monitor screen, to exclude as much ambient light as possible. Subjects dark-adapted for 15 minutes (MacLeod and Bartlett, 1954) prior to data collection, during which time, the apparatus was tested and practice trials were run. The experiment proper began once the variation within and between practice blocks of 32 trials for a single condition was consistent and small (see Figure 5, below).

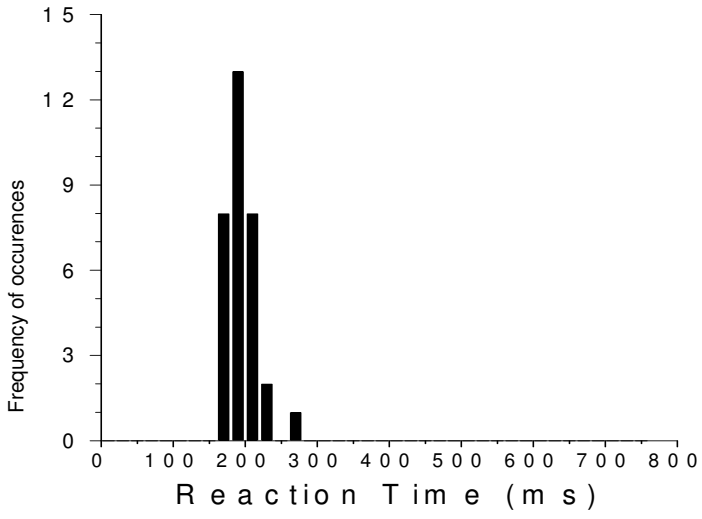

Figure 5. Typical block of trials with low inter-trial variability*. Here, mean ± SEM = 194.97 ± 3.68 ms.*

Manipulated stimulus parameters included luminance (L), spatial frequency (S), contrast (C), hemisphere, and eccentricity. Since foveal (0º) eccentricity was identical for LVF and RVF, there were thus seven stimulus positions (P), giving a total of 2 x 3 x 10 x 7 (420) combinations of stimulus parameters. For each of these combinations one *block* of 32 stimulus presentations was run. Subjects were tested on all positions and contrasts, and on three spatial frequencies (0.5, 1.73, 5.61 cpd) and two luminances (20, 0.2 $cd.m^{-2}$) (NH), or two spatial frequencies (0.5 and 5.61 cpd) and three luminances (20, 0.2, 0.02 $cd.m^{-2}$) (SP). Visual threshold for grating detection depended on the stimulus parameter combination. With low luminance, high spatial frequency and high eccentricity, only one or two contrast levels (0.5 and 0.2, say) were detectable. The actual number of conditions run, therefore, was far fewer than the theoretical maximum (420).

For each combination of luminance, spatial frequency, and position, up to ten contrast levels were tested. One block was run for each level, starting at C = 0.5. Subsequent blocks for each of the following contrast levels were run in order: C = 0.5, 0.2, 0.1, 0.08, 0.06, 0.04, 0.02, 0.01, 0.008, 0.006, until threshold (fewer than 20 responses) was reached. One further sub-threshold block was run (minimum contrast = 0.006), P, S, and L were altered, contrast was re-set to C = 0.5, and the next block began. Up to ten blocks of trials constituted a *set* of trials for each combination of L, S, and P. Subjects rested for a few minutes between sets.

There were several general rules governing set order. High luminance conditions were run first, on two separate days, and low luminance conditions were run on two further days. Within each luminance condition, foveal presentations for all spatial frequencies were run first. A typical stimulus presentation order is described below (Table 1).

Table 1. Set-presentation order for NH, illustrating general rules

Set (10x32 trials)	**L**	**P**	**S**	**Set** (10x32 trials)	**L**	**P**	**S**
1	20	0º	0.5	9	20	LVF 5º	5.61
2	20	0º	1.73	10	20	RVF 10º	0.5
3	20	0º	5.61				
4	20	RVF 5º	0.5	38	0.02	RVF 15º	1.73
5	20	RVF 5º	1.73	39	0.02	RVF 15º	5.61
6	20	RVF 5º	5.61	40	0.02	LVF 15º	0.5
7	20	LVF 5º	0.5	41	0.02	LVF 15º	1.73
8	20	LVF 5º	1.73	42	0.02	LVF 15º	5.61

10 blocks of 32 trials were run for each combination of luminance (L), position (P), and spatial frequency (S). Set = 10 blocks of 32 trials, RVF – right visual field, LVF – left visual field.

Forty-two sets were run for both subjects. Only the first ten and last five sets for NH are detailed in Table 1. Presentation of two (SP) or three (NH) sets of stimuli to one eccentricity was followed by a set to the same eccentricity in the opposite visual field. (i.e. RVF-5º was followed by LVF-5º). Additionally, all stimuli for any one eccentricity were run on the same day (e.g., for NH, all high luminance foveal and 5º stimuli were run on day 1, and all high luminance 10º and 15º stimuli were run on day 2).

Stimuli appeared on the monitor screen with a random foreperiod of between 1 and 3 seconds. If no response was made within 3 seconds of stimulus onset, a 100 ms tone sounded to indicate the beginning of the next foreperiod. Responses were followed by a 1-second interval before the beginning of the next foreperiod. Subjects maintained fixation on the appropriate fixation point, and responded as quickly and as accurately as possible, while refraining from anticipating the stimulus or making eye or head movements. Eye position and movement recordings were not made, and bite-boards and artificial pupils were not used. This is not uncommon for experiments requiring fixation. In similar experiments under identical viewing conditions (Plainis, 1999), pupil diameter for three subjects was measured at different screen luminances. Mean ± SEM pupillary area at 20, 0.2, and 0.02 $cd.m^{-2}$ screen luminance was 24.1 ± 0.6, 36.7 ± 2.3, and 42 ± 0.9 mm^2 respectively. This corresponds to a retinal illuminance at the three luminance levels of 482 ± 12, 7.3 ± 0.5, and 0.8 ± 0.02 Trolands (td) respectively.

3.5 Control experiments

Control experiments were run on NH as follows. Grating stimuli were set to a mean luminance of 20 $cd.m^{-2}$, spatial frequency of 0.5 cpd, and contrast of 0.5. Two blocks of 64 trials were run for each position, for responses made with both left and right hands, and with left and right feet (using the Treadlite foot pedal). Stimulus presentation order was constrained by the same rules as for the main experiments.

3.6 Data analysis

Each block generated 32 RT measurements. RTs below 150 ms (anticipation errors) and above 800 ms (omission errors) were excluded, as were RTs that fell outside the mean ± 2 standard deviations (on first-pass). Furthermore, all blocks that subsequently contained fewer than 20 (62.5 %) valid data were omitted and not further analysed. This was only the case for low-contrast blocks near visual threshold.

3.6.1 Error and variability

Anticipation and omission errors for all blocks except the lowest contrast block in each set were analysed as errors per block for the two subjects separately. Frequency of errors between subjects was compared with 2-tail t-tests across luminance conditions and subjects.

Data variability was assessed for both subjects by calculation of the coefficient of variation (CV = standard deviation / mean). The distribution of CV was analysed between subjects and luminances using 2-tail t-tests.

3.6.2 Control data

The data for NH's hand and foot responses for left and right response sides was averaged for each condition and compared by inspection. Differences between individual data points were analysed with 2-tail t-tests. The data was reduced to n = 80 (details in Section 4.2), and analysed with repeated measures ANOVAs with factors of position (7 levels), hemifield (2 levels), response limb (2 levels), and response side (2 levels). Further ANOVAs compared means for hands and feet and left and right sides separately.

3.6.3 Experimental data

Means and standard errors were calculated for each condition yielding >19 valid data. Results for sets of data were plot as a function of contrast, and compared between sets (4.3.1). Grand averages of all data collapsed over all conditions except luminance and each other condition were then obtained for left and right visual fields and subjects separately (4.3.2). Differences between LVF and RVF data were inspected visually and individual data points were compared with 2-tail t-tests where appropriate. Individual, un-collapsed data was compared for a small range of conditions as a function of spatial frequency. Since threshold was reached at different contrast levels for different conditions, ANOVA analyses on the complete data set were not valid or appropriate, due to the large data reduction that it would entail. Finally, the RT-contrast slope was linearised, and the regression slope coefficient computed for each condition. The slope coefficient was plotted for each subject separately as a function of eccentricity, for different spatial frequencies and luminances. The resulting ('space-ship') plots were inspected visually.

4. Results

All data in the text, unless otherwise stated, are expressed as mean ± the standard error of the mean (SEM) for all valid n. Statistical-test indices are given with degrees of freedom (df) subscripted (i.e. t_{df} and F_{df}). Reaction times and errors are given to 1 d.p., t-values to 3 d.p.

4.1 Errors

The number of valid RT data points for each block of trials above threshold was compared between luminance levels and subjects. Subject SP yielded significantly more valid data than NH (30.4 ± 0.1 vs. 25.9 ± 0.2; $t_{381} = 19.495$, $p < 0.0001$) in total, and for 0.02 ($t_{92} = 5.906$, $p < 0.0001$) and 20 cd.m^{-2} ($t_{242} = 16.48$, $p < 0.0001$) separately. Subject SP produced significantly more valid data for 0.2 compared to 0.02 cd.m^{-2} ($t_{76} = 2.175$, $p = 0.033$), and NH produced significantly more valid data for 0.02 compared to 20 cd.m^{-2} ($t_{206} = 4.752$, $p < 0.0001$). There were no significant differences between LVF and RVF valid data across luminance conditions for both NH and SP. Valid data points between different eccentricities and spatial frequencies were not analysed.

4.2 Data variability

There was a significant between-subjects difference in the coefficient of variation (CV) for both 0.02 (0.132 ± 0.003 vs. 0.106 ± 0.004; $t_{140} = 5.239$, $p < 0.0001$) and 20 cd.m^{-2} (0.183 ± 0.003 vs. 0.127 ± 0.004; $t_{326} = 11.099$, $p < 0.0001$). In both cases the CV for NH was higher than that for SP. Between-subject variability was not analysed across other conditions.

4.3 Control data

Figure 6 below shows the data for subject NH's left and right hand and foot RT to a grating (S = 0.5 cpd; C = 0.5; L = 20 cd.m^{-2}) at seven stimulus positions.

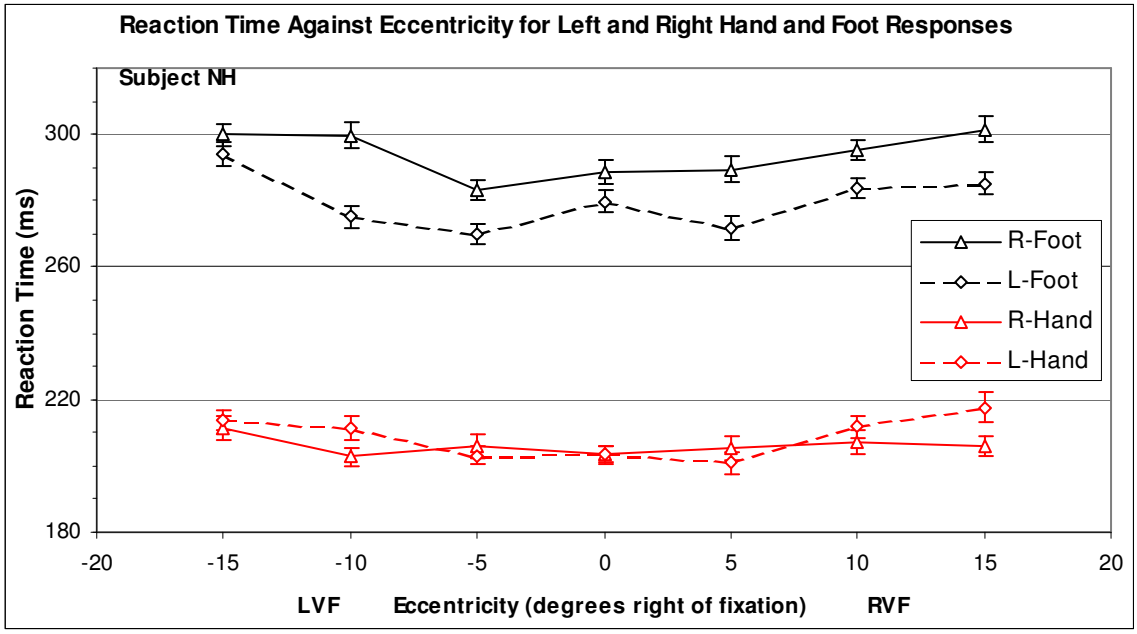

Figure 6. Left and right hand and foot reaction time for different stimulus positions*. The grating stimulus was of 0.5 cpd, at contrast = 0.5, and 20 cd.m^{-2} luminance. Black symbols and lines – foot responses; red symbols and lines – hand responses; triangles and solid lines – right limb; diamonds and broken lines – left limb. Data are mean ± SEM, 80 ≤ n ≤ 113.*

Several points can be made about the control results (Figure 6). The most obvious trend was the increased RT for responses made with the foot compared to the hand. The difference, comparing hands and feet on the same side of the body across eccentricity means was 79.4 ± 2.8 ms. The next most apparent trend was the consistent left foot over right foot RT advantage. The left foot response was on average 13.5 ± 2.5 ms faster than the right foot (mean of means across eccentricities).

4.3.1 ANOVA results

Of 128 responses per condition, an average of 96 ± 2.2 (range 80-113) were valid data. There were no significant differences between number of valid data for left and right sides, but there were significantly more valid data for hand compared to feet responses (102.7 ± 2.3 vs. 88.9 ± 2.8; $t_{26} = 3.867$, $p = 0.0007$), indicating increased error and variation for foot compared to hand responses. For an ANOVA on the RT data, 80 data were selected from each of the 28 conditions as follows. Conditions were assigned a random number for each data point, the random numbers were then sorted in descending order, and the first (n – 80) data were excluded. The remaining 80 data were subjected to a 3-way ANOVA, with factors of position (7 levels), response limb (2 levels), and response side (2 levels). All main and interaction effects were highly significant ($p < 0.001$). Hand responses were faster than foot responses (206.6 ± 3.8 ms, vs. 287.3 ± 3.6 ms; $F_1 = 13717.7$), responses with the left side were faster than with the right side (244 ± 3.6 ms, vs. 249.8 ± 3.8 ms; $F_1 = 704.1$), and the interaction of limb and response side ($F_1 = 1619.3$) shows that the difference between left and right sides was greater for feet than it was for hands. Separate 2-way ANOVAS for hand

and feet responses showed that the right hand was faster than the left (205.1 ± 3.9 ms, vs. 208.1 ± 3.8 ms; F_1 = 101.8, $p < 0.001$), and that the left foot was faster than the right (279.9 ± 3.5 ms, vs. 294.6 ± 3.7 ms; F_1 = 2076.1, $p < 0.001$).

Main and interaction effects of eccentricity were highly significant in the above analyses, but to characterise the effects of eccentricity *and* visual field, two further 3-way ANOVAs (eccentricity [3] x visual field [2] x response side [2]) were carried out for hand and foot responses separately. For hand responses there was no main effect of visual field ($F_1 = 0.499$, $p = 0.482$), but a main effect of eccentricity ($F_2 = 242.7$, $p < 0.001$) such that RT increased from 203.2 ± 3.7 ms at 5º, to 206.9 ± 3.8 ms at 10º, and 212.5 ± 3.9 ms at 15º. There were significant interaction effects with visual field as a factor, but these were difficult to interpret. In all cases, the F-values for these interactions were much lower than for other interactions due to the absence of a main effect of field. For foot responses, there was a significant main effect of field ($F_1 = 40.87$, $p < 0.001$), but the LVF advantage was only 1.55 ms across the conditions (compare the non-significant LVF advantage of 0.34 ms for hand responses). Reaction times for 5º, 10º, and 15º were 279.4 ± 3.5 ms, 288.9 ± 3.5 ms, and 295.6 ± 3.5 ms respectively, this trend being highly significant ($F_2 = 1750.6$, $p < 0.001$). There was a significant field-eccentricity interaction effect ($F_2 = 46.8$, $p < 0.001$), but again this was difficult to interpret.

4.4 Experimental Data

The largest variations in RT between conditions were produced by manipulation of stimulus luminance. For this reason, data from different luminance conditions are plotted separately throughout this section. Data were plotted on linear (RT) – log (contrast) scales to expand data at low contrast levels. On linear-linear scales, RT-contrast curves were hyperbolic (see Figure 14 below, and Section 5.3). Axis, scale, and symbol conventions apply throughout. Data is collapsed across conditions as detailed in the text.

4.4.1 Reaction time-stimulus relationships

Figures 7 and 8, below show data for subject NH and SP respectively. Reaction time (y-axis) against contrast (x-axis) was plotted for different eccentricities. All data in Figures 7 and 8 are for stimuli of 0.5 cpd, and collapsed across visual field.

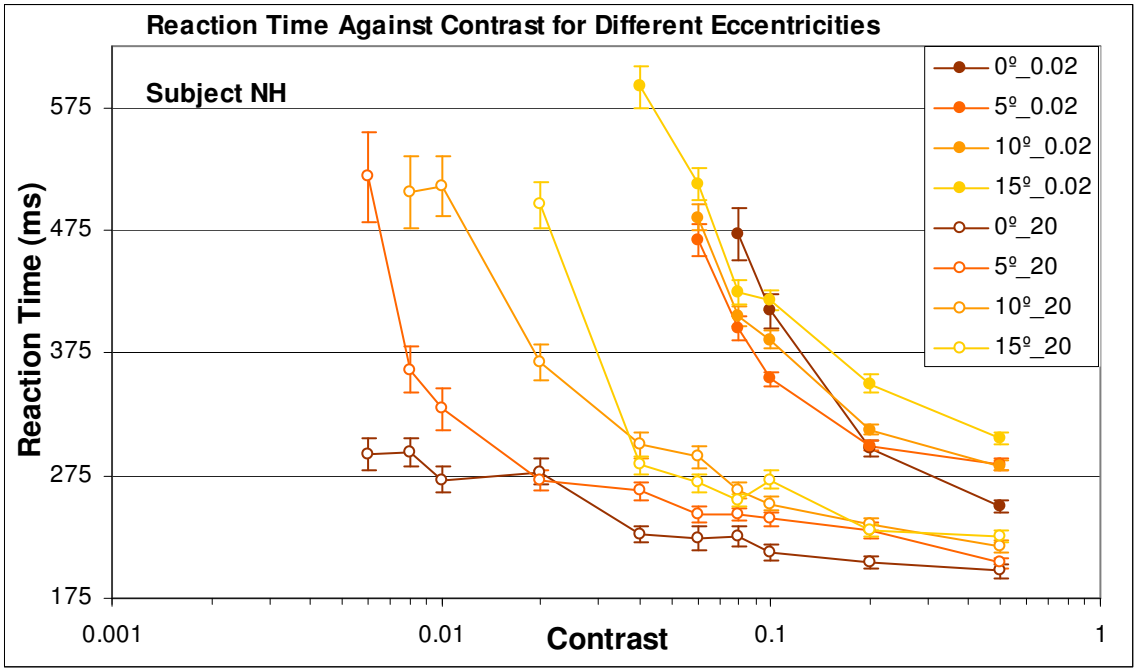

Figure 7. Reaction time against contrast for different eccentricities – Subject NH*. Foveal stimuli – dark orange; increasing eccentricities are in orange of increasing lightness (details in legend). Open circles – 20 cd.m^{-2}; Filled circles – 0.02 cd.m^{-2}. Data are mean ± SEM, collapsed*

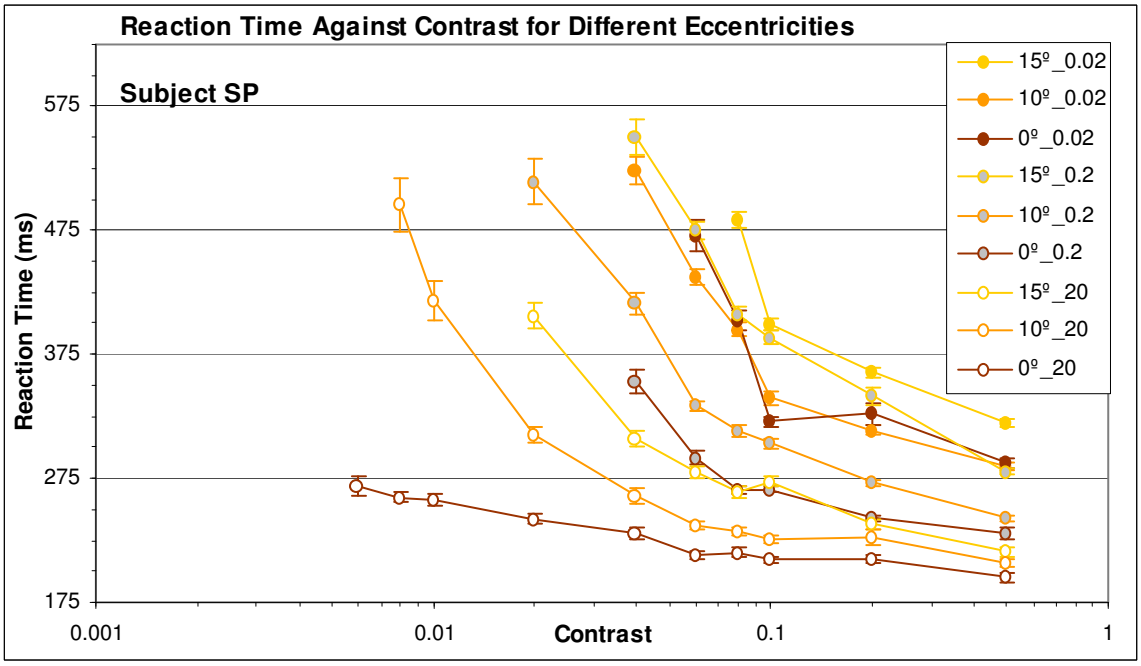

across LVF and RVF for eccentricities 5º, 10º, and 15º, 40 ≤ n ≤64. For foveal (0º), 20 ≤n ≤32.

Figure 8. Reaction time against contrast for different eccentricities – Subject SP*. Legend as Figure 7, except grey filled circles – 0.2 cd.m^{-2}. Data for 5º eccentricity are not shown for clarity. Data are mean ± SEM, collapsed across LVF and RVF. For eccentricities 10º and 15º, 40 ≤n ≤ 64. For foveal (0º), 20 ≤n ≤32.*

Figures 7 and 8 show several general trends. Firstly, RT increased monotonically with decreasing stimulus contrast. Secondly, data for different luminance levels were clearly separated, such that decreasing stimulus luminance increased both the absolute RT, and the RT-contrast slope. Thirdly, increasing eccentricity increased absolute RTs for all luminance levels, but increased the RT-contrast slope more for high luminance (20cd.m^{-2}) stimuli than for low luminance (0.02 and to a lesser extent 0.2 cd.m^{-2}) stimuli; RT-contrast slopes at low luminance were more parallel across eccentricities than at high luminance. Fourthly, apart from certain foveal, high luminance data, the lowest contrast level (i.e. threshold) had a RT consistently between 475 and 575 ms for both subjects.

Figures 9 and 10, below show data for subject NH and SP respectively. Reaction time against contrast was plotted for different spatial frequencies. All data in Figures 9 and 10 are for foveal stimuli.

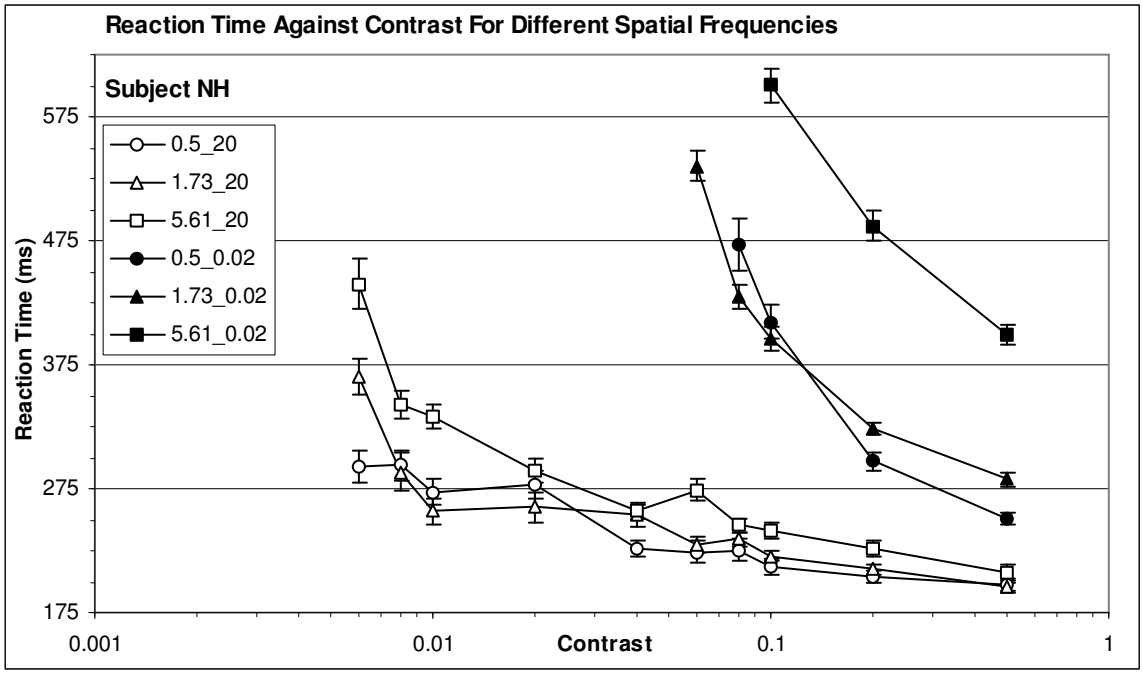

Figure 9. Reaction time against contrast for different spatial frequencies – Subject NH*. Circles – 0.5 cpd; triangles – 1.73 cpd; squares – 5.61 cpd; open symbols – 20 cd.m^{-2}; filled symbols – 0.02 cd.m^{-2}. Data are mean ± SEM for foveal stimuli, 20 ≤ n ≤ 32.*

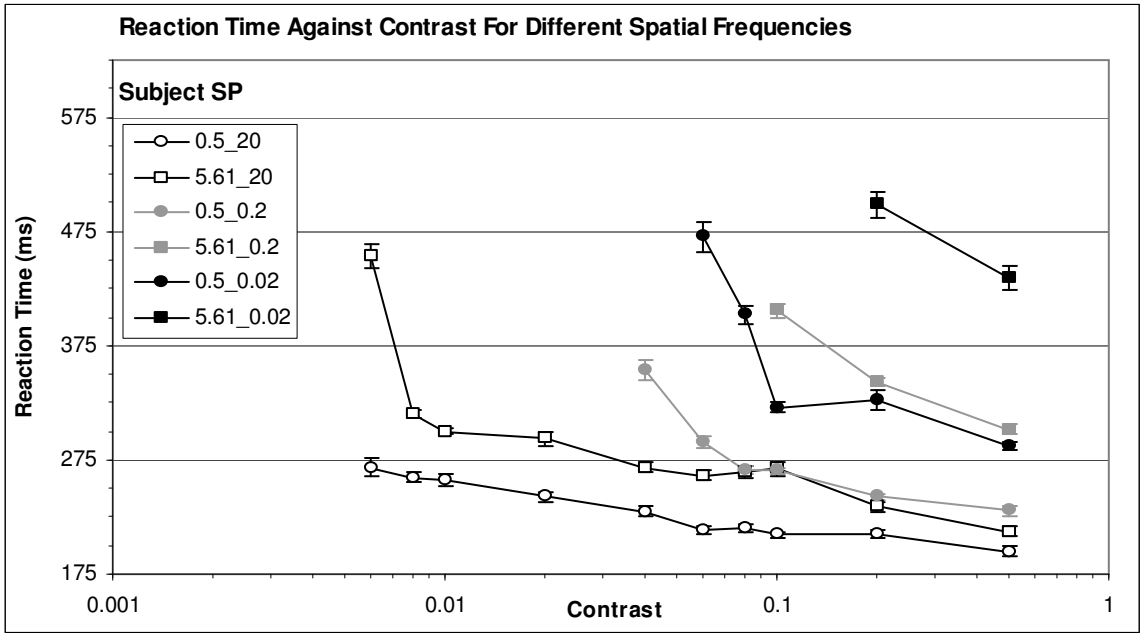

Figure 10. Reaction time against contrast for different spatial frequencies – subject SP*. Legend as Figure 9, except; grey filled circles – 0.2 cd.m^{-2}. Data are mean ± SEM for foveal stimuli, 20 ≤ n ≤32.*

As in Figures 7 and 8, RT increased monotonically with contrast for all conditions (Figures 9 and 10). This RT-contrast slope was steeper for low compared to high luminance conditions, and was marginally steeper for 5.61 cpd compared to 0.5 and 1.73 cpd at 20 cd.m^{-2} (by inspection). As spatial frequency increased and luminance decreased, absolute RT increased for all conditions. There was an overlap in SP's data for mid- and low-luminance conditions, such that RTs for stimuli of 5.61 cpd at 0.2 cd.m^{-2} were longer than for stimuli of 0.5 cpd at 0.02 cd.m^{-2}.

4.4.2 Hemispheric processing

To detect any general trends with respect to asymmetrical response speed, data were collapsed over all conditions except contrast. The following Figures 11 and 12 show data for all 5050 (NH) and 4948 (SP) observations respectively, with decreasing n for stimulus conditions nearing threshold.

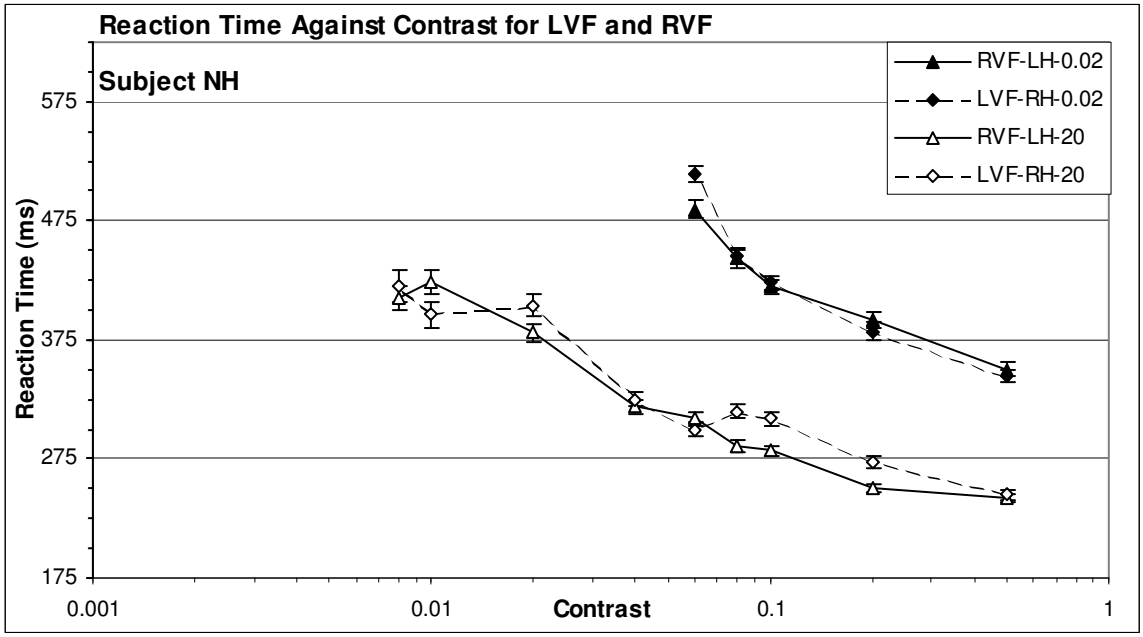

Figure 11. Reaction time against contrast for LVF and RVF stimuli – Subject NH*. Open symbols – 20 cd.m^{-2}; filled symbols – 0.02 cd.m^{-2}; triangles and solid lines – RVF; diamonds and broken lines – LVF. Data are mean ± SEM, 45 ≤ n ≤ 238.*

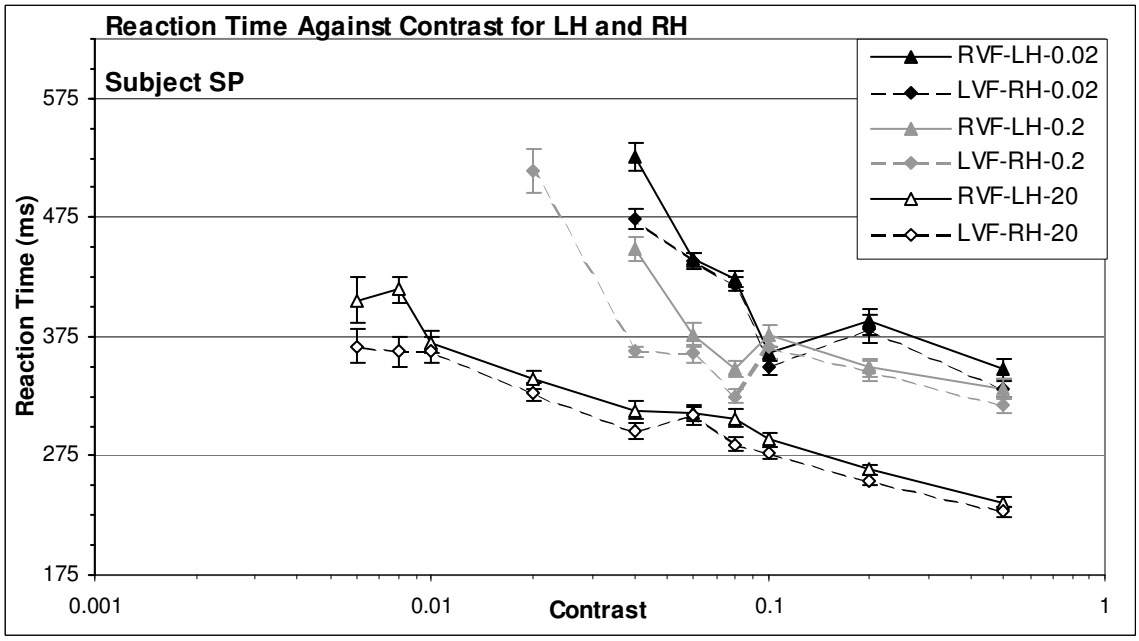

Figure 12. Reaction time against contrast for LVF and RVF stimuli – Subject SP*. Legend as Figure 11, except; grey filled symbols – 0.2 cd.m^{-2}. Data are mean ± SEM, 20 ≤ n ≤ 185.*

For subject NH (Figure 11), there was no apparent hemispheric RT-asymmetry except for the lowest contrast at 0.02 cd.m^{-2}, and for three high contrast points (C = 0.2, 0.1, and 0.08) at 20 cd.m^{-2}. For each of these 20 cd.m^{-2} points, RT was significantly lower for RVF stimuli (t_{424} = 3.373, p = 0.0008; t_{416} = 3.383, p = 0.0008; t_{424} = 3.787, p = 0.0002

respectively). For subject SP, on the other hand, a striking trend was apparent. For every point, RTs were shorter for stimuli presented in the LVF. At the lowest, this LVF advantage was 0.91 ms (C = 0.06; L = 0.02 cd.m^{-2}), while the maximum was 86.1 ms (C = 0.04; L = 0.2 cd.m^{-2}). The mean LVF advantage was 19.1 ± 4.4 ms.

To determine if the general trends of Figures 11 and 12 could be a function of stimulus parameters other than contrast, the data sets were re-analysed for both subjects, and are presented below as a function of spatial frequency (NH only, Figure 13).

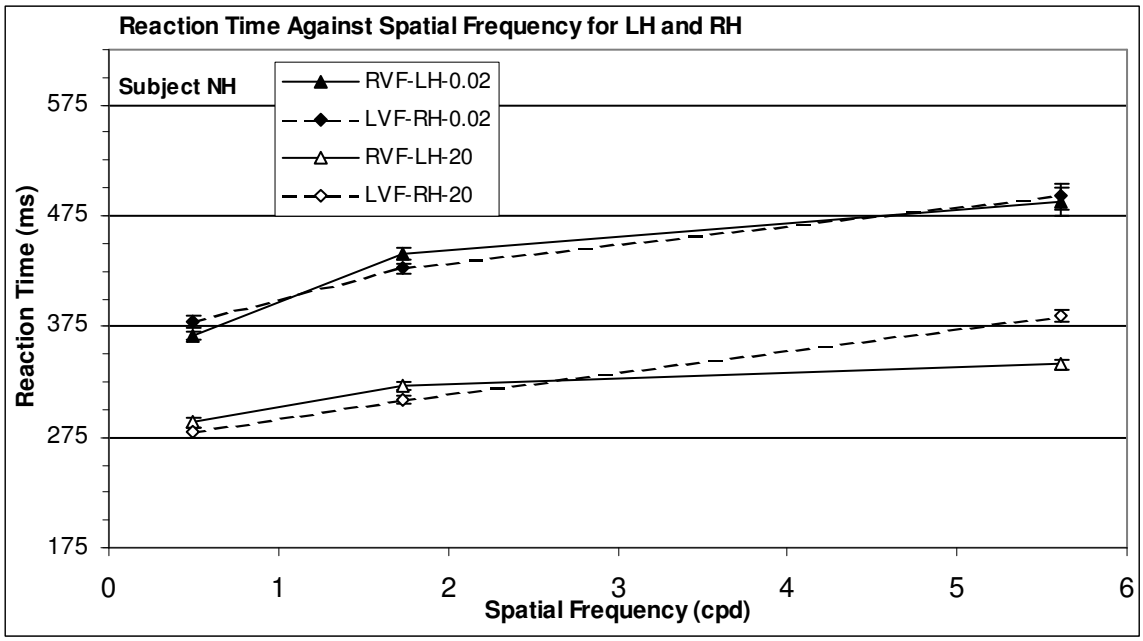

Figure 13. Reaction time against spatial frequency for LVF and RVF stimuli - subject NH. *Open symbols – 20 cd.m-2; filled symbols – 0.02 cd.m-2; triangles and solid lines – RVF; diamonds and broken lines – LVF. Data are mean ± SEM, 75 ≤ n ≤ 666.*

Subject NH showed no consistent trend towards hemispheric asymmetries across luminances, however at 20 cd.m^{-2} RTs were significantly lower for 5.61 cpd RVF stimuli (340.6 ± 4.2, vs. 384.8 ± 5.2 ms; $t_{844} = 6.478$, $p < 0.0001$). The difference at 0.5 cpd was non-significant, and at 1.73 cpd was just significant ($t_{1248} = 2.231$, $p = 0.02$), while at 0.02 cd.m^{-2}, both 0.5 and 1.73 were bordering on significance ($t_{815} = 2.023$, $p = 0.043$; $t_{734} = 1.936$, $p = 0.053$ respectively). Overall, there was no consistent trend for low luminance data, but for the high luminance data, a trend in the direction of the spatial frequency hypothesis was apparent. This is discussed further below (5.3).

For subject SP (data not shown), in all cases RTs were lower for LVF stimuli. The mean difference between means across spatial frequencies and luminances was 13.6 ± 3.4 ms (range 3.5 – 26.9 ms).

Data was re-analysed for both subjects, comparing LVF and RVF stimuli at different eccentricities and luminances. The same general remarks can be made about this data (not shown) as were made for contrast (Figures 11 and 12) and spatial frequency (Figure 13). Subject NH was faster for RVF stimuli at 5º at both 0.02 (not significant) and 20 $cd.m^{-2}$ ($t_{1317} = 3.549$, $p = 0.0004$), and faster for LVF stimuli at 15º for both luminances (non-significant). Subject SP was faster for LVF stimuli at all eccentricities, the mean difference was 14.7 ± 3.4 ms (range 3.58 – 28.2 ms). Standard errors ranged from 3.3 – 7.8 ms, suggesting many of these differences would be highly significant (not tested).

At different luminances, NH was non-significantly faster for RVF stimuli at both 0.02 (RVF advantage = 2.0 ms) and 20 $cd.m^{-2}$ (RVF advantage = 4.5 ms). Subject SP was consistently and significantly faster for LVF stimuli at all luminances ($t_{1018} = 2.157$, $p = 0.031$; $t_{1379} = 4.269$, $p < 0.0001$; $t_{2676} = 4.313$, $p < 0.0001$, for 0.02, 0.2, and 20 $cd.m^{-2}$ respectively). The mean LVF advantage was 16.5 ± 2.8 ms (range 12.6 – 22.0).

In addition to the results presented above, where data were collapsed over stimulus conditions, separate plots of RT against spatial frequency were made for different eccentricities and two contrast levels (C = 0.5 and 0.2) for both subjects (data not shown). These plots confirmed that subject SP showed a consistent LVF advantage on virtually all data points, and exclude the possibility that this advantage was an artefact of the collapsed-averaging process. The plots for NH showed no consistent trends over the same stimulus parameters, and few statistically significant differences.

4.4.3 RT-Contrast relationship

Figure 14 below shows a range of data chosen to represent a large range of stimulus parameters and levels, and including data from both subjects.

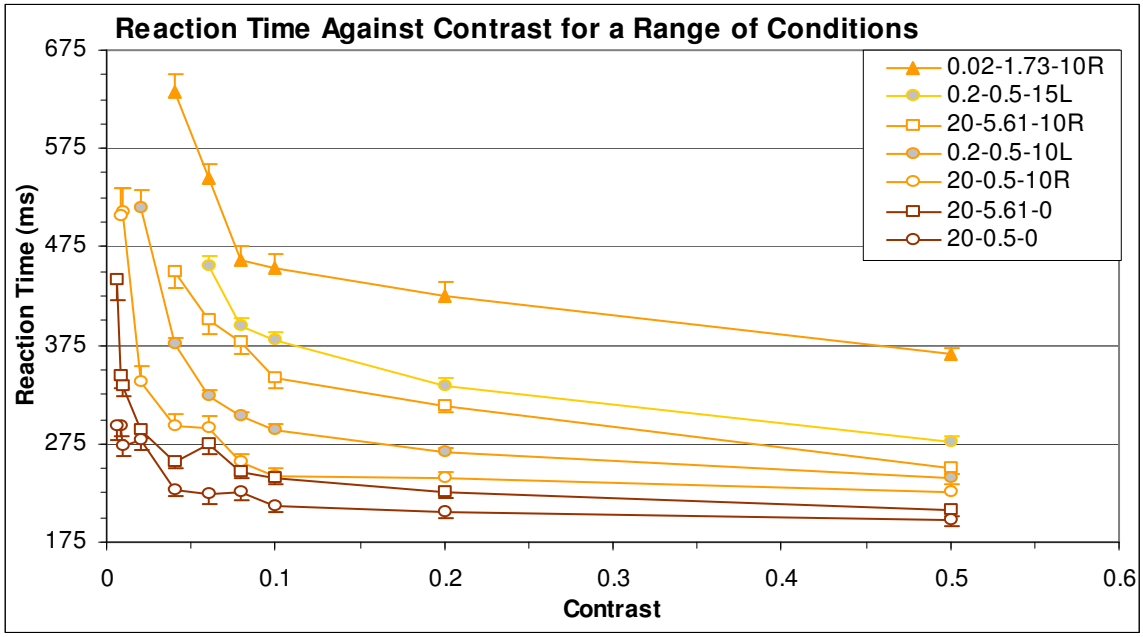

Figure 14. Reaction time against contrast for a wide range of stimulus conditions*. Data are taken from both subjects, and from at least one of each stimulus condition levels. Legend labels: Luminance-Spatial Frequency-EccentricityHemifield (L-S-EH). Circles – 0.5 cpd; triangles – 1.73 cpd; squares – 5.61 cpd. Foveal stimuli – dark orange; increasing eccentricities are in orange of increasing lightness (details in legend). R – RVF; L – LVF. Open circles – 20 cd.m^{-2}; grey filled circles – 0.2 cd.m^{-2}; filled circles – 0.02 cd.m^{-2}. Data are mean ± SEM, 20 ≤ n ≤ 32.*

It is apparent that the RT-contrast curves may approximate to a hyperbolic function of contrast, that is

$$RT = (m / C) + k \qquad \text{(Equation 2)}$$

Where; RT = reaction time (y-axis), m = hyperbolic slope coefficient, C = contrast (x-axis), k = constant

If this relationship holds, then plotting RT against the reciprocal of contrast should linearise the RT-contrast slope. Algebraically:

$$RT = (m / C^{-1}) + k \qquad \text{(Equation 3)}$$

$$RT = mC + k \qquad \text{(Equation 4)}$$

Where m is the linear slope coefficient and k is the y-axis intercept, which corresponds to the RT asymptote of the RT-contrast plot.

Figure 15 below shows the RT-1/Contrast (RT-C^{-1}) plot for the same range of data as in Figure 14. This plot clearly shows the linear relationship between RT and the reciprocal of contrast.

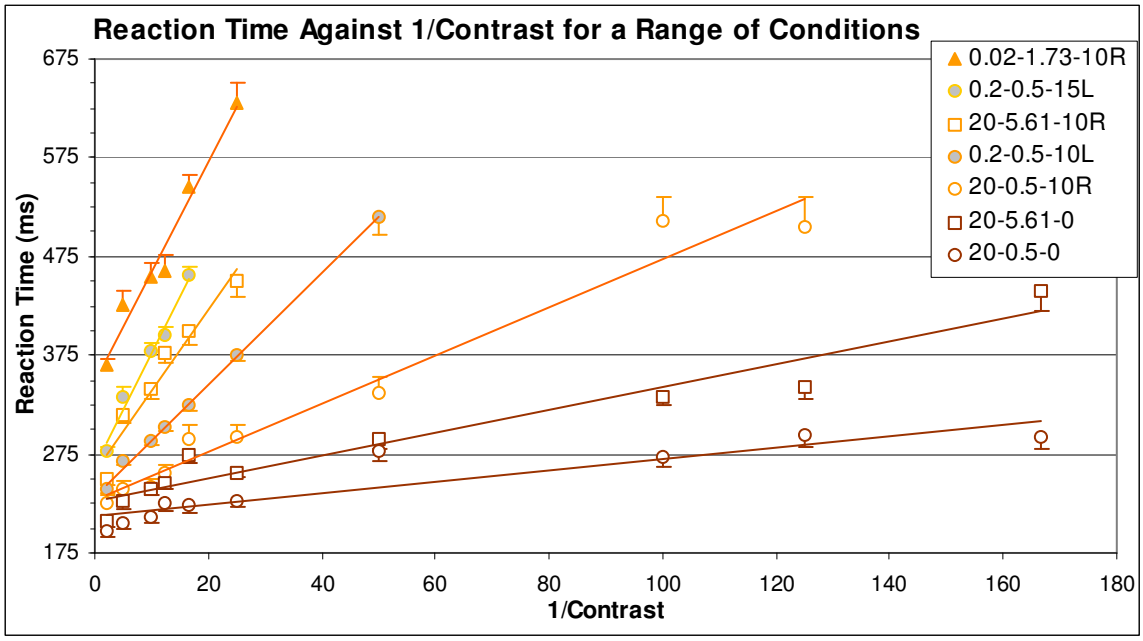

Figure 15. Reaction time against the reciprocal of contrast for a wide range of stimulus conditions. *Data are taken from both subjects. Legend as Figure 14. Data are mean ± SEM, 20 ≤ n ≤ 32.*

The linear relationship held for a wide range of stimuli. All data were transformed by plotting RT against the reciprocal of contrast, and subjected to a linear regression analysis to obtain the RT on 1/contrast regression equation (e.g. Figure 15). Each RT-1/contrast plot yielded a regression slope, a RT-intercept, and an r-squared value. Over 35 (31) stimulus sets (set = 10 x 32 trials), the mean r-squared value for NH (SP) was 0.926 ± 0.012 (0.948 ± 0.01). This difference in r-squared values between subjects was non-significant ($t_{63} = 1.367$, $p = 0.176$).

Figures 16 and 17, below show the RT-C^{-1} slope for subjects NH and SP respectively, for all conditions as a function of eccentricity.

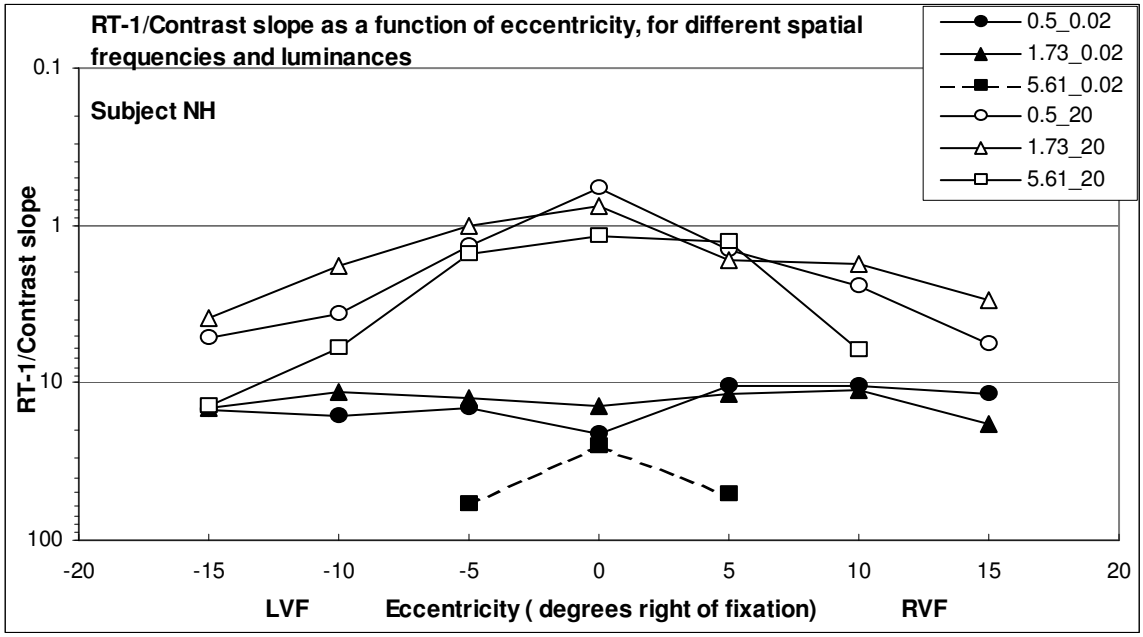

Figure 16. Reaction time-1/contrast slope against stimulus position for different spatial frequencies and luminances – subject NH*. Each data point represents the slope of the regression equation of RT on 1/contrast, for a set of stimuli over a range of contrasts. Circles – 0.5 cpd; triangles – 1.73 cpd; squares – 5.61 cpd. Open symbols – 20 cd.m-2; filled symbols – 0.02 cd.m-2. Solid lines – slope derived from n ≥ 3 contrast levels; broken lines – slope derived from 2 contrast levels only (referring to the more eccentric point). Total n = 5050. Note the reversed scale on the y-axis, showing increasing RT-1/contrast slope from top to bottom. The x-axis is scaled to represent the visual field topographically.*

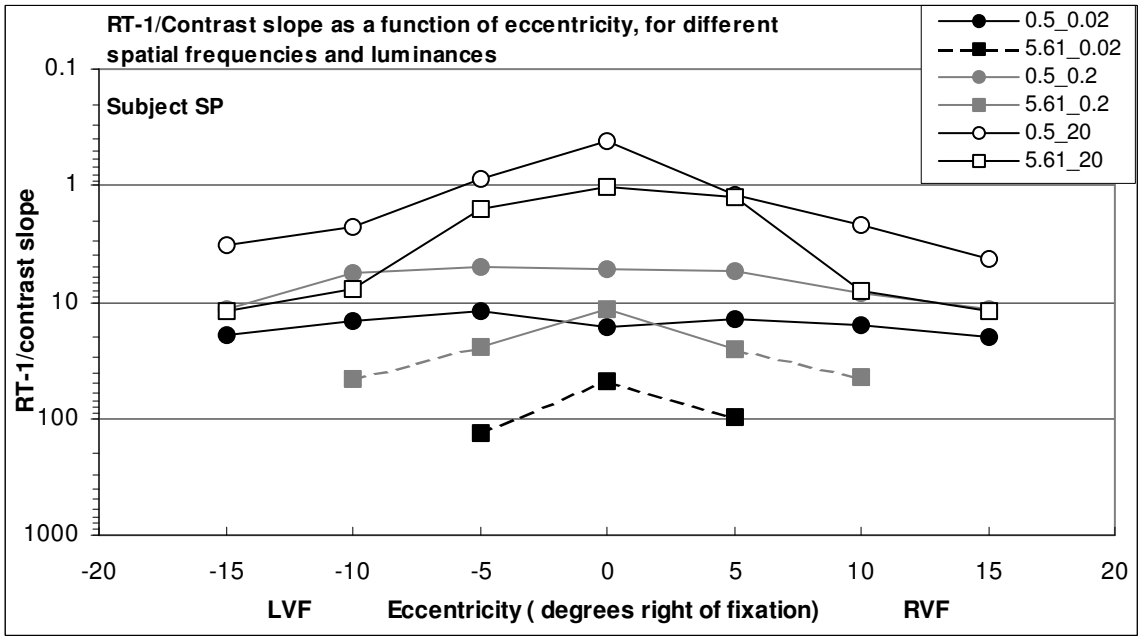

Figure 17. Reaction time-1/contrast slope against stimulus position for different spatial frequencies and luminances – subject SP. *Each data point represents the slope of the regression equation of RT on 1/contrast, for a set of stimuli over a range of suprathreshold contrasts. Legend as Figure 16. Total n = 4948. Note the reversed scale on the y-axis, showing increasing RT-1/contrast slope from top to bottom. The x-axis is scaled to represent the visual field topographically.*

Figures 16 and 17 show several important features. Firstly, RT-C^{-1} slopes increased with decreasing luminance. Secondly, with increasing eccentricity, 20 cd.m^{-2} stimuli showed a greater modulation in RT-C^{-1} slope than 0.2 or 0.02 cd.m^{-2} stimuli. Thirdly, 5.61 cpd stimuli showed a greater increase in RT-C^{-1} slope with eccentricity than 0.5 and 1.73 cpd stimuli for all luminance levels. Fourthly, for NH, 1.73 cpd RT-C^{-1} slopes were shallower than 0.5 cpd slopes. This trend is not predictable from analysis of RT data alone, since RTs to 0.5 cpd are consistently faster than RTs to 1.73 cpd stimuli. Finally, and perhaps most striking, there was a remarkable and aesthetic symmetry to the data – a quality that has earned this plot the nickname 'the Space-Ship graph'. While there were several hemifield / hemispheric asymmetries worthy of note (e.g. the increased LVF compared to RVF slopes for 0.5 cpd at 0.02 cd.m^{-2}, and the decreased 5º LVF compared to 5º RVF slope for 1.73 cpd at 20 cd.m^{-2} for NH), in general, and considering that each 'space-ship' plots only one subject's data, there was an impressive symmetry.

The RT-C^{-1} intercepts were plotted on the same axes as Figures 16 and 17. These plots (not shown) also showed systematic differences as a function of stimulus eccentricity, spatial frequency, and luminance. In general, RT-C^{-1} intercepts increased with increasing eccentricity and spatial frequency and with decreasing luminance. There was much overlap between plots, however, and the relationships were not as clear as in Figures 16 and 17.

5. Discussion

The aims of the present study were threefold. 1. To characterise the relationship between simple reaction time and the spatial and luminance characteristics of sinusoidal gratings over a range of stimulus values. 2. To determine if there were any systematic processing asymmetries between stimuli presented in left and right visual fields, and whether these asymmetries were a function of the stimulus characteristics. 3. To derive a linear coefficient that describes the RT-contrast relationship over a wide range of conditions, and to assess if there were any systematic hemispheric asymmetries with respect to this variable. Each of these aims will be looked at in detail below, after a discussion of error, variability and control data.

5.1 *Error, variability, and control data*

Subject SP, a highly practised subject, yielded significantly more valid data points than NH, who was performing SRT tasks for the first time. Furthermore, the coefficient of variation for SP was significantly lower than for NH. The r-squared value for the RT-C^{-1} plots was non-significantly higher for SP than for NH. These measures suggest that SP's data is intrinsically more reliable both between and within stimulus conditions. Inter-subject variability is not uncommon in SRT paradigms (see Greenlee and Breitmeyer, 1989).

Control data showed that RTs made with the hands were on average 79.4 ms faster than for the feet (Figure 6). There are several possible reasons for this difference. Firstly, an experimental artefact may have confounded the result – foot responses were collected with a foot pedal, while hand responses were collected with a small button. The excursion of the pedal (approximately 1 cm at the apex) prior to effecting contact with the trigger switch was longer than that for the button (approximately 5 mm). This will have introduced a constant difference between hand and foot responses, presumably due to the increased biomechanical excursion of the limbs in order to respond. To determine this difference, one further control experiment is required – using the foot pedal to make *manual* responses under identical conditions. Unfortunately, this control experiment was not carried out.

Secondly, the feet are approximately 1 m (for NH, height = 186 cm) further from the brain than are the hands. This increased distance is traversed by motoneurones descending in corticospinal tracts of the ventral spinal columns, and synapsing at lumbar-sacral levels. Primary motoneurons originating in the ventral horn of the spinal cord then conduct the impulse to effector muscles in the lower leg. Assuming a nervous conduction velocity of between 30 and 130 ms^{-1} for A-fibres (Tortora and Anagnostakos, 1990), the extra time required to effect the response over 1 metre will be between 8 and 33 ms.

Thirdly, the cortico-motor connectivity of pathways subserving finger movements is qualitatively different from those subserving distal leg responses. The cortico-motoneuronal (CM) pathways project from primary motor cortex, and synapse directly onto motoneurones serving muscles of the fingers and hand. Pathways subserving lower limb motor control, however, are poly-synaptic and not as highly specialised as the CM pathways (Lemon, 1995). This will introduce further conduction delay. Thus, hand/finger responses are likely to be faster even when biomechanical excursion and conduction times are taken into account (see also the discussion of unilateral / bilateral control of musculature; DiStefano *et al*., 1980).

An intriguing finding from the control results was that, for all stimulus positions, left foot responses were on average 13.5 ms faster than right foot responses. This difference was present regardless of the visual field in which the stimulus was presented. The dissociation between left and right foot RT, independent of visual field or stimulus parameters, suggests either that the effect is an artefact of the experimental conditions, or that there is a perceptual-motor hemispheric asymmetry which is specific to the feet. The first possibility cannot be ruled out without replication of the present results under similar and dissimilar stimulus conditions. Practise and fatigue effects can be ruled out, since for every data point, left and right response collection was alternated. Furthermore, at the end of the control session, the two initial data points (foveal stimuli, left and right feet response) were replicated and yielded distributions of RTs that were not significantly different from the original data set.

The second possibility is more interesting, and suggests either that the transformation of perceptual information into a motor response, or the motor response itself, is differentially slowed for the right foot with respect to the left. This is not discussed further here.

Overall, the control results show that, for right and left hand responses, there were no systematic, easily interpretable SRT differences for stimuli presented in either visual field.

5.2 *Simple reaction time to sinusoidal gratings: effect of stimulus manipulations*

Four stimulus parameters were manipulated: contrast, eccentricity (or position), spatial frequency, and luminance. As contrast decreased from C = 0.5, RT increased monotonically for all stimulus conditions (Figures 7, 8, 9, 10). Reaction time was related to contrast by a hyperbolic function of the form RT = (m / C) + k (Equation 2), where m is the hyperbolic slope coefficient, and k is a constant, representing the RT-asymptote. The value of m and k varied as a function of the stimulus conditions. With increasing eccentricity, both m and k increased, such that the RT-asymptote increased, and the rate of increasing RT with decreasing contrast also increased. In Figures 7 and 8, this is seen for 20 $cd.m^{-2}$ stimuli as the upward shift in the RT asymptote (from around 200 to 225 ms), and the increasing slope of the RT-contrast curve for 0º, 5º, 10º, and 15º stimuli respectively.

For different luminance levels, both m and k increased with decreasing luminance (note the upwards shift with decreasing luminance for comparable stimuli on all RT-contrast plots, and the steeper function for low luminances). For low luminances (0.2 and 0.02 $cd.m^{-2}$), m did not increase with increasing eccentricity as much as for high luminance (20 $cd.m^{-1}$) stimuli, however, k increased monotonically (plot not shown) with increasing eccentricity (see Figures 7 and 8). Mansfield (1973) and Rains (1963) studied visual reaction times for light flashes of different intensity, duration, and position. These authors reported a RT asymptote of around 200 ms for photopic, and 240 ms for scotopic luminance stimuli. These findings comport well with the present data.

A similar relationship held for increasing spatial frequency as for eccentricity, namely, as spatial frequency increased, both m and k increased. This relationship was clear for comparisons between 0.5 and 5.61 cpd, and between 1.73 and 5.61 cpd, but not between 0.5 and 1.73 cpd. This difference can be explained with reference to the transient and sustained channel dichotomy (see Section 5.4, below). If high spatial frequencies are processed by the sustained channels (long latency, small receptive fields), and low spatial frequencies by the transient channels (short latency, large receptive fields), then reaction times will increase with increasing spatial frequency (Lupp *et al*., 1976). One caveat to bear in mind when interpreting the data for different spatial frequencies, is the fact that contrast sensitivity is significantly decreased for sinusoidal gratings with fewer than four complete luminance cycles (Hoekstra *et al*., 1974, see also Kelly, 1975; Savoy and McCann, 1975). For the 0.5 cpd condition, with a stimulus size of 7º of visual angle, only 3.5 cycles are available. This is a possible confound.

What can be said about the upper and lower limits of the RT-contrast plots? At the lower end of the range, with increasing contrast RT decreased and began to plateau. Whether RT had reached an asymptote for the fastest responses (20 $cd.m^{-2}$, 0.5 cpd, 0º) is arguable, but with contrast on a log scale it appeared close to, but not at, asymptote when C = 0.5 (Figures 7, 8 and 14). With lower luminance levels, it was clear that RT had not reached asymptote at C = 0.5. Further research should be directed at verifying the contrast level at which asymptote is reached, and also in correlating the RT at this asymptote with the k value predicted from the calculated RT-contrast equation.

The upper bound of the RT-contrast plot refers to the visual threshold for contrast sensitivity. Threshold was not directly measured in the present study, so only rough assertions can be made about its relation to RTs. For stimulus conditions in which threshold was reached before the last contrast level (i.e. threshold > C = 0.006), the threshold RT was consistently between 475 and 575 ms (see Figures 7 and 8). For some conditions, threshold contrast yielded RTs as low as 350 ms (Figure 8), however it is likely that these contrast levels were 'further' from actual threshold than for the conditions yielding longer 'threshold' RTs. The relationship between threshold contrast and RT was not investigated here, but see 5.4 below.

5.3 Hemispheric processing of sinusoidal gratings

For subject NH, for data both collapsed across conditions and treated separately, there were no overall systematic trends towards differential processing of stimuli between the hemispheres. That is, there were no systematic LVF or RVF advantages in RT to sinusoidal gratings. At various specific conditions, such as at C = 0.2, 0.1, and 0.08 (collapsed data, Figure11), there was a significant RVF-LH advantage for high luminance (20 $cd.m^{-2}$) stimuli. At 20 $cd.m^{-2}$, NH showed a LVF-RH advantage for low spatial frequencies, and a RVF-LH advantage for high spatial frequencies. This dissociation is in the direction predicted by the spatial frequency hypothesis (Sergent, 1983). The high spatial frequency advantage was 44 ms in favour of the LH. This is a very large difference for a SRT paradigm, and is discussed below.

We must be cautious about drawing conclusions from the present data, based on an individual subject's results. A problem of interpretation throughout the present study is that, as stimulus parameters moved towards threshold (increasing spatial frequency and eccentricity, decreasing contrast and luminance), fewer and fewer data were available at the different stimulus levels. This situation was necessary in order to characterise the near- and supra-threshold RT-stimulus relationship, crucial to the present aims. Given that NH produced more variable and fewer valid data per condition than SP, we should not be surprised to find highly significant differences at several individual data points. It is not strictly valid, therefore, to draw conclusions about trends across conditions with large differences in the number of data points.

Separate plots of the collapsed data for different eccentricities and luminances for NH also failed to yield a consistent trend, though high variability was again apparent. Similarly, plotting data that was not collapsed across conditions showed no systematic hemifield differences (for 3 eccentricities, 2 luminances, and 2 contrast levels, data not shown).

In striking contrast, subject SP showed a highly consistent and significant trend towards a LVF-RH advantage on virtually every condition, whether the data was collapsed across conditions or not. The mean, SEM, and range of LVF-RH advantages for collapsed data is presented in Table 2, below.

Table 2. Mean LVF-RH RT advantages for data collapsed over conditions – subject SP

		LVF-RH Advantage (ms)			
Variable	**N**	**mean**	**SEM**	**min**	**max**
Contrast	22	19.1	4.4	0.9	86.1
Eccentricity	9	14.7	3.4	3.6	28.2
Spatial Frequency	6	13.6	3.4	3.5	26.9

Luminance	3	16.5	2.8	12.6	22.0

Values show mean ± SEM, and range of RVF-LVF RT differences over collapsed data for different conditions. Data for Contrast, Eccentricity, and Spatial Frequency were plotted for separate luminances.

The possible confounds of order, practice, and fatigue presumably can be ruled out, since left and right conditions were alternated, and the testing occurred over four separate days with all LVF and RVF comparison conditions tested on the same day. The possible effect of non-random stimulus presentations within blocks is discussed below.

Davis and Graham (1981) manipulated the probability of occurrence of sinusoidal gratings, in a task where subjects had to say in which of two temporal intervals a near-threshold grating had appeared, regardless of its spatial frequency. These authors found that, as the probability of occurrence of a particular spatial frequency increased, the detection threshold for that grating decreased while thresholds for other gratings increased. Thus, without receiving explicit instructions to attend to particular spatial frequencies, the detection of more probable spatial frequencies was facilitated. Their findings were extended to a wider range of spatial frequencies and retinal loci (Davis *et al*., 1983), and a similar study showed comparable results in cats (Martens and Blake, 1980), who have CSFs similar to those of humans (Enroth-Cugell and Robson, 1966; Daitch and Green, 1969). These results can be interpreted in terms of an attentional modulation of the input channels required for the detection of different spatial frequencies.

This is a controversial conclusion, however, since it is assumed that input channels of (visual) processing are not the domain of attentional mechanisms (according to the modularity thesis; Fodor, 1983, and see Moran and Desimone, 1985 and Corbetta *et al*., 1990 for single unit and PET studies respectively). Some recent research has supported the notion of attentional modulation of early processing, however. Fink and colleagues (1996) showed significant *pre-striate* activity in an attentional task similar to Navons' (1977) hierarchical letters task (see Figure 1). Furthermore, a compelling report published last year (Benedetti *et al*., 1999), recorded target-specific activation of opioids in *spinal cord* somatotopic maps, contingent on the subject's *expectation* of analgesia delivered to the represented body part. This shows attentional modulation of early processing *par excellence*!

Could attentional factors have played a part in the present study? Blocks of trials involved only one spatial frequency at a time. It is therefore possible that expectation effects could have influenced target detection. The spatial frequency hypothesis predicts that attentional mechanisms bias the LH in favour of high spatial

frequencies and the RH in favour of low spatial frequencies. This may have occurred here in the limited case discussed above of the collapsed data for NH. Subject SP, however, showed a LVF-RH advantage on all conditions regardless of spatial frequency. In this case, if attentional mechanisms are at work, then is it plausible that there could be an attentional bias for LVF-RH detection of stimuli regardless of specific stimulus conditions?

As mentioned in the introduction (2), SRT paradigms with lateralised light flashes and other simple stimuli, consistently yield LVF-RH advantage of varying statistical significance. Right visual field / left hemisphere advantages are also reported, but they are fewer in number. Importantly, the magnitude of published LVF-RH advantages range from 1.3 to 10 ms. The present data for SP show LVF-RH advantages of 13 to 19 ms. Given that the LVF-RH advantages in the published studies are derived from more than one subject and given as mean values, the present values do not differ greatly from the published results, especially given that the majority of published LVF-RH advantages are between 3 and 8 ms. There is certainly cause to replicate the data for SP.

Braun and colleagues (1996) suggested that SRT studies consistently, although non-significantly, showed a LH-high luminance, RH-low luminance dissociation. On careful inspection of all available graphs for both collapsed data and data from separate conditions, no support for their assertion was found. The present findings cast doubt on the asymmetries reported in their paper, and their speculation of a neuroanatomical substrate for this asymmetry.

5.4 The RT-contrast relationship across eccentricity, luminance and spatial frequency

When reaction time was plotted against the reciprocal of contrast, the hyperbolic RT-contrast slope was linearised, and this linearity held for a wide range of stimulus conditions (Figures 14 and 15; see also Plainis *et al*., 1999; Plainis and Murray, 2000). The plot of the RT-C^{-1} slope coefficient, apart from having aesthetic appeal, highlights some important features of the early processing of sinusoidal visual stimuli. Firstly, at high luminances, the increase in RT as a function of decreasing contrast was smallest at the fovea, and increased monotonically with eccentricity. Secondly, this increase in slope was greater for high spatial frequencies than for low spatial frequencies. These two properties can be explained with reference to the density of cells in the retino-striate pathway. High luminance (20 $cd.m^{-2}$) stimuli are above the receptor threshold sensitivity for retinal cone receptors. Thus, cones will transduce the high luminance signals, and will constrain their processing accordingly. The distribution of cones throughout the retina is not uniform. The highest density of cones is in the fovea and central 0.18º (Curcio *et al*., 1990), while receptor density decreases rapidly in all directions radial from the fovea. The distribution of cones along the horizontal meridian for both nasal and temporal hemiretinae is shown in Figure 18, below. Cone density is 40% higher at equivalent eccentricities in the nasal compared to the temporal hemiretina (Curcio *et al*., 1990).

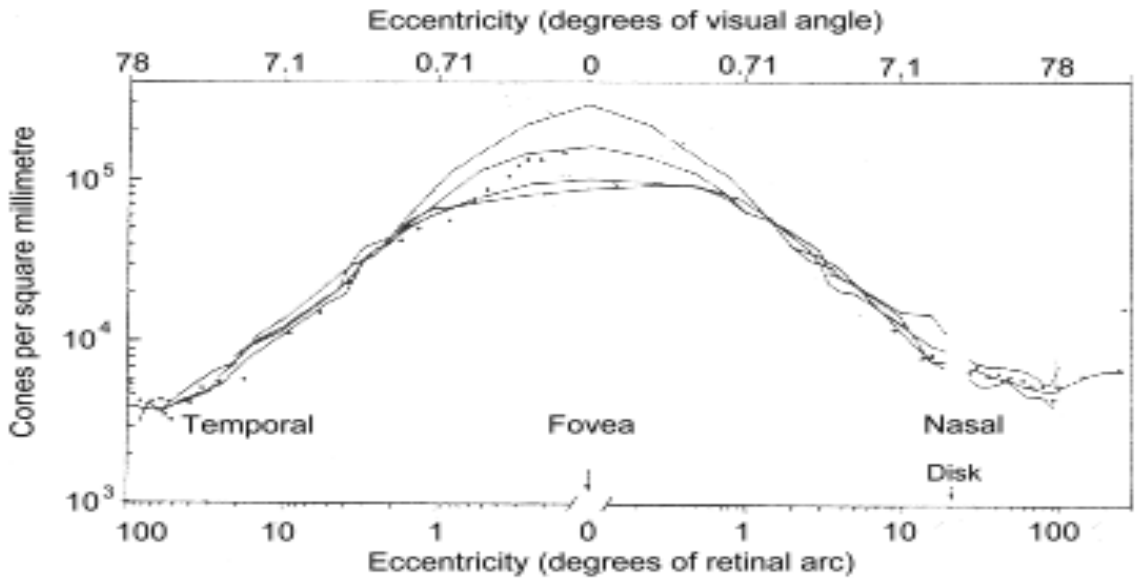

Figure 18. The distribution of cone receptor cells along the horizontal meridian of the retina**. The left side of the plot shows the temporal hemiretina, and the right side the nasal hemiretina. Different lines show data from the retinae of different human subjects. Note the log-log scale, and the general shape of the curve. Adapted from Curcio *et al*., 1987.**

The decreasing density of cone receptors with increasing eccentricity can also account for the greater decrease in RT-C^{-1} slope for high compared to low spatial frequencies. As receptor density decreases, so too does the resolving power of the visual system, such that high spatial frequencies will become progressively harder to detect. With increasing eccentricity, optical characteristics of the eye also reduce the availability of high spatial frequencies (Campbell and Robson, 1968). In general, with increasing eccentricity, the loss of high spatial frequency information is greater than for low spatial frequencies (see also Polich, 1978; Christman, 1990).

The above characteristics of retinal photoreceptor cell density are paralleled and amplified by the entire retino-striate projection. When the cortical magnification factor (the number of striate cortical cells that serve to represent each square degree of visual angle, encompassing receptor density and neural convergence; Green, 1970) is taken into account, the reduction in contrast sensitivity for eccentricities up to 30º from the fovea is completely accounted for (Rovamo *et al*., 1978). This finding suggests that, with respect to contrast, spatial frequency, and eccentricity, early visual processing is functionally homogenous.

The situation for the low (0.02 $cd.m^{-2}$) luminance level is qualitatively different. For 0.5 and 1.73 cpd, the $RT\text{-}C^{-1}$ slope does not increase with increasing eccentricity, rather it remains fairly constant. Again, this can be accounted for by recourse to retinal cell distribution. Rod receptors are uniquely operative at retinal illuminances of below 1 td (Plainis, 2000, personal communication). The 0.02 $cd.m^{-2}$ condition in experiments similar to those presented here produced, for three subjects, a mean retinal illuminance of 0.8 ± 0.02 td. Thus, we can be fairly sure that stimulus energy at the lowest luminance level was transduced exclusively by rod receptors. Rod receptor density is more uniform across the retina than cone receptor density. Rod cell density peaks at about 18º eccentricity (Curcio *et al*., 1990), and falls off gradually either side. The absence of rods in the *fovea centralis* may have produced the slight 'dip' seen in the 0.02 $cd.m^{-2}$ conditions for foveal stimuli for both subjects (Figures 16 and 17). The large (7º) target was still visible when presented at zero eccentricity, however, since rod receptors are first present at 0.63º eccentricity (Curcio *et al*, 1990) and the grating stimuli extended to 3.5º in all directions from foveal fixation. In summary, response sensitivity at different eccentricities correlates well with both rod and cone receptor cell density (Rains, 1963; Mansfield, 1973; Hilz and Cavonius, 1974).

At the level of the retinal ganglion cells, and the subsequent geniculo-striate projections, different 'channels' have been distinguished (Cleland *et al*., 1971, 1973; Kulikowski and Tolhurst, 1973; Breitmeyer, 1975; Lupp *et al*., 1976). Retinal ganglion X cells have small receptive fields, are sensitive to blur (removal of high spatial frequency information), relatively insensitive to temporal modulations of stimuli, have long response latencies, and are concentrated in the fovea. On the other hand, Y-cells have large receptive fields, are insensitive to blur, but sensitive to temporally-modulated stimuli, have short response latencies, and are relatively more abundant in the peripheral retina. These properties strongly suggest that X-cells are specialised to process high spatial frequency information, and Y-cells low spatial frequencies. These cell types give rise to the sustained and transient channels respectively.

A neuroanatomical characterisation of retinal ganglion cells makes the distinction between parvocellular cells (P-cells) on the one hand, and magnocellular cells (M-cells) on the other. P-cells are small (Latin *parvus* = small; *magnus* = large), have low retino-geniculate conduction velocity, do not function well at scotopic luminance, and have low luminance contrast gain. M-cells are large, have high retino-geniculate conduction velocity, function at scotopic luminance, and have high contrast gain (Kaplan, 1989). Other P- and M-cell characteristics parallel those for X- and Y-cells respectively, and the two distinctions are thought to pertain to overlapping populations of cells and channels.

For the $RT\text{-}C^{-1}$ plots, the scotopic luminance data may reflect transient channel, retinal ganglion Y-cell, and M-cell activity (hereafter the 'T-Y-M system'). The high luminance $RT\text{-}C^{-1}$ plots reflect the operation of

both classes of process, depending on the stimulus characteristics. Thus, for foveal, high spatial frequency targets, both systems (the T-Y-M system, and the sustained channel, retinal ganglion X-cell, and P-cell system – hereafter the 'S-X-P system'[5]) are operative, and RT will depend on the system that provides the shortest latency neurophysiological response. For low spatial frequencies, this is provided by the T-Y-M system, and results in a short latency response. For high spatial frequencies, the latency at the fovea may be more dependent on the S-X-P system. Longer latencies for high compared to low spatial frequencies, and steeper RT-C^{-1} slopes will result (compare the foveal, high luminance plots for both subjects in Figures 16 and 17).

The above considerations apply equally to the 0.2 $cd.m^{-2}$ luminance level for SP's data. Since this luminance was not at scotopic, pure rod-vision levels, it reflects an intermediate level between 20 and 0.02 $cd.m^{-2}$. As is clearly apparent from Figure 17, the RT-C^{-1} slope coefficient data is also intermediate with respect to that for the higher and lower luminance levels.

As eccentricity increases and luminance decreases, the contribution of the short-latency T-Y-M system is increasingly relied upon. For low spatial frequencies, this results in a lesser attenuation in response latency than it does for high spatial frequencies, since the transient channels, upon which high spatial frequency responses are increasingly dependent, are not sensitive to high spatial frequency information.

Plainis and Murray (2000) have shown that the RT-C^{-1} slope coefficient predicts both contrast sensitivity and contrast gain in single-cell studies on macaque P- and M- retinal ganglion cells. The RT-C^{-1} slope coefficient is related to contrast gain by a reciprocal function, and predicts perceived contrast for a wide range of stimulus spatial frequencies and retinal illuminances. Discussion of this aspect is deferred to another report (Holmes *et al*., 2000). Further studies should evaluate the effect of stimulus *duration* on hemispheric asymmetries in SRT over a wide range of contrasts and spatial frequencies. This variable was not manipulated in the present study, but other data (Plainis and Murray, 2000) suggests that stimulus duration affects the RT-C^{-1} slope coefficient in ways predictable with reference to the primate contrast gain and contrast sensitivity. Short stimulus durations will tend to favour the transient channels, and therefore low spatial frequencies (Lupp *et al*, 1976).

[5] Note that this distinction between T-Y-M and S-X-P systems is not absolute or rigid, and is used here for expediency.

6. Conclusions

In assessing hemispheric asymmetries in the processing of sinusoidal gratings in simple reaction time paradigms, it may be preferable to compare not RT data directly, but a linear slope coefficient derived from the plot of RT against the reciprocal of contrast. This measure is preferable since it provides a value that is independent of specific contrast levels or specific reaction times. Rather, this measure relates the change in RT contingent on a change in contrast for a sinusoidal grating of given spatial frequency, eccentricity, and luminance. The RT-C^{-1} slope coefficient is inversely proportional to some characteristics of input-level visual pathway neurones as studied in macaque models, namely contrast sensitivity and contrast gain. If functional hemispheric asymmetries are related to attentional modulation of neural processing, and if it is assumed that input pathways are not attentionally-modulated, then the RT-C^{-1} slope coefficient is an ideal measure by which to evaluate functional asymmetries in SRT paradigms. In the present study, the RT-C^{-1} slope coefficient was remarkably consistent between and within subjects and hemispheres, whereas absolute RT values showed large significant differences and inter-subject variability.

7. Acknowledgements

For expert supervision, hours of detecting gratings and a constant supply of cakes and fresh coffee, thanks go to Dr Sotiris Plainis of The Optometry and Neuroscience Department, UMIST. For accepting me into his department, and casting an experienced eye over the experimentation and data, Dr Ian Murray, also of UMIST was a great help. Thanks are due to Dr Nuala Brady of The University of Manchester Department of Psychology, for always being available for friendly advice and enthusiasm. Dr Neil RA Parry developed the reaction time software. I didn't get to meet him.

8. References

Anzola GP, Bertoloni G, Buchtel HA, Rizzolatti G. (1977). Spatial Compatibility and Anatomical Factors in Simple and Choice Reaction Time. *Neuropsychologia*, **15** : 295 - 302

Benedetti F, Arduino C, Amanzio M, (1999). Somatotopic Activation of Opioid Systems by Target-Directed Expectations of Analgesia. *The Journal of Neuroscience*, **19** : 3639 – 3648

Berlucchi G, Crea F, Di Stefano M, Tassinari G. (1977). Influence of Spatial Stimulus-Response Compatability on Reaction Time of Ipsilateral and Contralateral Hand to Lateralised Light Stimuli. *Journal of Experimental Psychology: Human Perception and Performance*, **3** : 505 - 517

Braun CMJ, Daigneault S. (1994). Effects of a Right Hemifield Advantage on Crossed-Uncrossed Differentials in Simple Reaction Time: Towards a New Model of Interhemispheric Relay. *Acta Psychologia*, **85** : 91 - 98

Braun CMJ, Mailhoux C, Dufresne A. (1996). Left and Right Visual Field Advantages are a Function of Scotopic and Photopic Retinal Adaptation, Respectively, in Simple Reaction Time to Near-Threshold Targets. *Acta Psychologica*, **91** : 3 - 14

Brady N, Field DJ. (1995). What's Constant in Contrast Constancy? The Effects of Scaling on the Perceived Contrast of Bandpass Patterns. *Vision Research*, **35**: 739 - 756

Breitmeyer BG. (1975). Simple Reaction Time as a Measure of the Temporal Response Properties of Transient and Sustained Channels. *Vision Research*, **15** : 1411 - 1412

Brown WS, Barsz K, Sprecher E, Emmerlich DS. (1984). Laterality Effects in Response to the Offset of Visual Stimuli. *Neuropsychologia*, **22** : 627 - 629

Bryngdahl O. (1966). Perceived Contrast Variation with Eccentricity of Spatial Sine-Wave Stimuli. *Vision Research*, **6** : 553 - 565

Campbell FW. (1980). The Physics of Visual Perception. *Philosophical Transactions of the Royal Society of London B*, **290** : 5 - 9

Campbell FW, Green DG. (1965). Monocular Versus Binocular Visual Acuity. *Nature*, **208** : 191 -192

Campbell FW, Maffei L. (1975). Contrast and Spatial Frequency. *Scientific American*, **231 (5)** : 106 - 114

Campbell FW, Robson JG. (1968). Application of Fourier Analysis to the Visibility of Gratings. *Journal of Physiology*, **197** : 551 - 566

Christman S. (1990). Effects of Luminance and Blur on Hemispheric Asymmetries in Temporal Integration. *Neuropsychologia*, **28** : 361 - 374

Christman S, Kitterle FL, Hellige J. (1991). Hemispheric Asymmetry in the Processing of Absolute versus Relative Spatial Frequency. *Brain and Cognition*, **16** : 62 - 73

Clarke JM, Zaidel E. (1989). Simple Reaction Times to Lateralised Light Flashes. *Brain*, **112 :** 849 - 870

Cleland BG, Dubin MW, Levick WR. (1971). Sustained and Transient Neurones in the Cat's Retina and Lateral Geniculate Nucleus. *Journal of Physiology*, **217** : 473 - 496

Cleland BG, Levick WR, Sanderson KJ. (1973). Properties of Sustained and Transient Ganglion Cells in the Cat Retina. *Journal of Physiology*, **228** : 649 - 680

Corbetta L, Miezen FM, Dobmeyer S, Shulman GL, Petersen SE. (1990). Attentional Modulation of Neural Processing of Shape, Colour, and Velocity in Humans. *Science*, **: 248** : 1556 - 1559

Curcio CA, Sloan KR, Kalina RE, Hendrickson AE. (1990). Human Photoreceptor Topography. *Journal of Comparative Neurology*, **292** : 497 - 523

Curcio CA, Sloan KR Jr., Packer O, Hendrickson AE, Kalina RE. (1987). Distribution of Cones in Human and Monkey Retina: Invidual Variability and Radial Asymmetry. *Science*, **236** : 579 - 582

Daitch JM, Green DG. (1969). Contrast Sensitivity of the Human Peripheral Retina. *Vision Research*, **9** : 947 - 952

Davidoff JB. (1977). Hemispheric Differences in Dot Detection. *Cortex*, **13** : 434 - 444

Davis ET, Graham N. (1981). Spatial Frequency Uncertainty Effects in the Detection of Sinusoidal Gratings. *Vision Research*, **21** : 705 – 712

Davis ET, Kramer P, Graham N. (1983). Uncertainty About Spatial Frequency, Spatial Position, or Contrast of Visual Patterns. *Perception and Psychophysics*, **33** : 20 - 28

De Valois RL, Albrecht DG, Thorell LG. (1982). Spatial Frequency Selectivity of Cells in Macaque Visual Cortex. *Vision Research*, **22** : 545 - 559

Di Stefano M, Morelli M, Berlucchi G. (1980). Hemispheric Control of Unilateral and Bilateral Movements of Proximal and Distal Parts of the Arm as Inferred from Simple Reaction Time to Lateralised Light Stimuli in Man. *Experimental Brain Research*, **38** : 197 - 204

Enroth-Cugell C, Robson JG. (1966). The Contrast Sensitivity of Retinal Ganglion Cells of the Cat. *Journal of Physiology*, **187** : 517 - 552

Fendrich R, Gazzaniga M. (1990). Hemispheric Processing of Spatial Frequencies in Two Commissurotomy Patients. *Neuropsychologia*, **28** : 657 - 664

Fink GR, Halligan PW, Marshall JC, Frith CD, Fackowiak RSJ, Dolan RJ. (1996). Where in the Brain Does Visual Attention Select the Forest and the Trees? *Nature*, **382** : 626 - 628

Fiorentini A, Beradi N. (1984). Right Hemisphere Superiority in the Discrimination of Spatial Phase. *Perception*, **13** : 695 - 708

Fodor JA (1983). *The Modularity of Mind: An Essay on Faculty Psychology*. MIT Press, Cambridge

Franzén O. (1975). Apparent Contrast as a Function of Modulation Depth and Spatial Frequency. *Vision Research*, **15** : 655 - 660

Georgeson MA, Sullivan GD. (1975). Contrast Constancy: Deblurring in Human Vision by Spatial Frequency Channels. *Journal of Physiology*, **252** : 627 - 656

Green DG. (1970). Regional Variations in the Visual Acuity for Interference Fringes on the Retina. *Journal of Physiology*, **207** : 351 - 356

Greenlee MW, Breitmeyer BG. (1989). A Choice Reaction Time Analysis of Spatial Frequency Deiscrimination. *Vision Research*, **29** : 1575 - 1586

Haber and Hershenson (1989), cited by Plainis SP. (2000), personal communication

Harwerth RS, Levi DM. (1978). Reaction Time as a Measure of Suprathreshold Grating Detection. *Vision Research*, **18** : 1579 – 1586

Hellige JB, Sergent J. (1986). Role of Task Factors in Visual Field Asymmetries. *Brain and Cognition*, **5** : 200 - 222

Hilz R, Cavonius CR. (1974). Functional Organisation of the Peripheral Retina: Sensitivity to Periodic Stimuli. *Vision Research*, **14** : 1333 - 1337

Hoekstra J, van der Goot DPJ, van den Brink G, Bilsen FA. (1974). The Influence of the Number of Cycles upon the Visual Contrast Threshold for Spatial Sine-Wave Patterns. *Vision Research*, **14** : 365 - 368

Holmes NP, Plainis S, Murray IJ. (2000). Reaction Times as a Behavioural Measure of Contrast Gain: Comparison of Low and High Luminance Levels and Different Eccentricities. *Perception*, **29** (Supplement) : 78b. Paper presented at the ECVP Conference, Groningen, the Netherlands, 27th to 31st August

Ivry RB, Robertson LC. (1998). *The Two Sides of Perception*. MIT Press, London

Kaplan (1989), cited by Plainis SP. (2000), personal communication

Kelly DH. (1975). How Many Bars Make a Grating? *Vision Research*, **15** : 625 - 626

Kinchla RA, Wolfe JM. (1979). The Order of Visual Processing: "Top-Down," "Bottom-Up," or "Middle-Out." *Perception and Psychophysics*, **25** : 225 - 231

Kitterle FL. (1986). Psychophysics of Lateral Tachistoscopic Presentation. *Brain and Cognition*, **5** : 131 - 162

Kitterle FL, Kaye RS. (1985). Hemispheric Symmetry in Contrast and Orientation Sensitivity. *Perception and Psychophysics*, **37** : 391 - 396

Kitterle FL, Selig LM. (1991). Visual Field Effects in the Discrimination of sine-Wave Gratings. *Perception and Psychophysics*, **50** : 15 - 18

Kitterle FL, Christman S, Hellige JB. (1990). Hemispheric Differences are found in the Identification, but not the Detection of Low Versus High Spatial Frequencies. *Perception and Psychophysics*, **48** : 297 - 306

Kitterle FL, Hellige JB, Christman S. (1992). Visual Hemisphere Asymmetries Depend on Which Spatial Frequencies are Task Relevant. *Brain and Cognition*, **20** : 308 - 314

Kroon JN, Rijsdijk JP, van der Wildt GJ. (1980). Peripheral Contrast Sensitivity for Sine-Wave Gratings and Single Periods. *Vision Research*, **22** : 243 -

Kulikowski JJ. (1976). Effective Contrast Constancy and Linearity of Contrast Sensation. *Vision Research*, **16** : 1419 - 1431

Kulikowski JJ, Tolhurst DJ. (1973). Psychophysical Evidence for Sustained and Transient Detectors in Human Vision. *Journal of Physiology*, **232** : 149 – 162

Lemon RN. (1995). Cortical control of Skilled Movements. In Cody FWJ, (ed.). *Neural Control of Skilled Human Movement*, pp 1-11. Portland Press, London

Lines CR, Milner AD. (1983). Nasotemporal Overlap in the Human Retina Investigated by Means f Simple Reaction Time to Lateralised Light Flashes. *Experimental Brain Research*, **50** : 166 - 172

Lines CR, Rugg MD, Milner AD. (1984). The Effect of Stimulus Intensity on Visual Evoked Potential Estimates of Interhemispheric Transmission Time. *Experimental Brain Research*, **57** : 89 - 98

Lupp U, Hauske G, Wolf W. (1976). Perceptual Latencies to Sinusoidal Gratings. *Vision Research*, **16** : 969

- 972

MacLeod S, Bartlett NR. (1954). Human Reaction Time During Dark Adaptation. *Journal of the Optical Society of America*, **44** : 374 - 379

Mansfield RJW. (1973). Latency Functions in Human Vision. *Vision Research*, **13** : 2219 - 2234

Marshall JC, Halligan PW. (1995). Seeing the forest but Only Half the Trees. *Nature*, **373** : 521 - 523

Martens W, Blake R. (1980). Uncertainty Impairs Grating Detection Performance in the Cat. *Perception and Psychophysics*, **27** : 229 - 231

Martin M. (1979). Local and Global Processing: The Role of Sparsity. *Memory and Cognition*, **7** : 476 - 484

McKeever WF, Hoff AL. (1979). Evidence of a Possible Isolation of Left Hemisphere Visual and Motor Areas in Sinstrals Employing an Inverted Handwriting Posture. *Neuropsychologia*, **17** : 445 - 455

Michelson (1927). Cited by Campbell and Robson, 1968

Moran J, Desimone R. (1985). Selective Attention Gates Visual Processing in the Extrastriate Cortex. *Science*, **229** : 782 - 784

Murray IJ, Plainis S. (2000). A General Equation for Reaction Times to Contrast, Spatial Frequency and Luminance. Paper presented at the ARVO Conference, May, 2000

Navon D. (1977). Forest Before Trees: The Precedence of Global Features in Visual Perception. *Cognitive Psychology*, **9** : 353 - 383

Niebauer CL, Christman SD. (1999). Visual Field Differences in Spatial Frequency Discrimination. Brain and Cognition **41,** 381–389

Peterzell DH. (1991). On the Nonrelation Between Spatial Frequency and Cerebral Hemispheric Competence. *Brain and Cognition*, **15** : 62 - 68

Peterzell DH, Harvey LO Jr., Hardyck CD. (1989). Spatial Frequencies and the Cerebral Hemispheres: Contrast Sensitivity, Visible Persistence, and Letter Classification. *Perception and Psychophysics*, **46** : 443 - 455

Plainis S. (1999). Vision at Low Lighting Levels and Its Relation to Driving. PhD Doctoral Dissertation, UMIST, Manchester

Plainis S, Murray IJ. (2000). Reaction Times Predict Human Contrast Sensitivities and Contrast Gain in Single Unit Studies. Paper presented at the ARVO Conference, May, 2000

Plainis S, Murray IJ, Chauhan K, Charman WN. (1999). Reaction Times as an index of Visual Conspicuity at Night. Paper presented to the VIV 8 Conference, Boston, August

Polich JM. (1978). Hemispheric Differences in Stimulus Identification. *Perception and Psychophysics*, **24** : 49 - 57

Polster MR, Rapcsak SZ. (1994). Hierarchical Stimuli and Hemispheric Specialisation: Two Case Studies. *Cortex*, **30** : 487 - 497

Proverbio AM, Zani A, Avella C. (1997). Hemispheric Asymmetries for Spatial Frequency Discrimination in a Selective Attention Task. *Brain and Cognition*, **34** : 311 - 320

Rains JD. (1963). Signal Luminance and Position Effects in Human Reaction Time. *Vision Research*, **3** : 239 - 251

Rao SM, Rourke D, Whitman RD. (1981). Spatio-Temporal Discrimination of Frequency in the Right and Left Visual Fields: A Preliminary Report. *Perceptual and Motor Skills*, **53** : 311 - 316

Rijsdijk JP, Kroon JN, van der Wildt GJ. (1980). Contrast Sensitivity as a Function of Position on the

Retina. *Vision Research*, **20** : 235 - 241

Rose D. (1983). An Investigation into Hemispheric Differences in Adaptation to Contrast. *Perception and Psychophysics*, **34** : 89 - 95

Rovamo J, Virsu V, Näsänen R. (1978). Cortical Magnification Factor Predicts the Photopic Contrast Sensitivity of Peripheral Vision. *Nature*, **271** : 54 - 56

Savoy RL, McCann JL. (1975). Visibility of Low Spatial Frequency Sine-Wave Targets: Dependence on Number of Cycles. *Journal of the Optical Society of America*, **65** : 343 - 350

Sergent J. (1983). Role of the Input in Visual Hemispheric Asymmetries. *Psychological Bulletin*, **93** : 481 - 512

Tortora GJ, Anagnostakos NP. (1990). *Principles of Anatomy and Physiology*. *Sixth Edition*. Harper and Row, London

van Kleek MH. (1989). Hemispheric Differences in Global Versus Local Processing of Hierarchical Visual Stimuli by Normal Subjects: New Data and a Meta-Analysis of Previous Studies. *Neuropsychologia*, **27** : 1165 - 1178

Yund EW, Efron R, Nichols DR. (1990). Detectability Gradients as a Function of Target Location. *Brain and Cognition*, **12** : 1 – 16